GEOLOGICA BELGICA (2010) 13/4: 459-482

# TRACE ELEMENT VARIATIONS IN THE MIDDLE FRASNIAN *PUNCTATA* ZONE (LATE DEVONIAN) IN THE WESTERN CANADA SEDIMENTARY BASIN – CHANGES IN OCEANIC BIOPRODUCTIVITY AND PALEOREDOX SPURRED BY A PULSE OF TERRESTRIAL AFFORESTATION?

Maciej G. ŚLIWIŃSKI[1], Michael T. WHALEN[1] & Jed DAY[2]

(9 figures, 4 tables, 1 appendix)

[1]*Department of Geology & Geophysics, University of Alaska Fairbanks, Fairbanks, Alaska 99775, U.S.A.*
[2]*Department of Geography-Geology, Illinois State University, Normal, IL 61790-4400, USA*

**ABSTRACT.** The '*punctata* Event' (Early–Middle Frasnian transition, Late Devonian) was recently recognized as yet another episode of major geochemical perturbations associated with the Middle-Late Devonian ecosystem readjustments which culminated in the Frasnian-Fammenian (F/F) mass extinction event, one of five largest of the Phanerozoic. We report variations in total organic carbon (TOC), magnetic susceptibility (MS), major, minor and trace element proxies (for changes in detrital input, bioproductivity and redox conditions) across the *P.punctata* conodont biozone in the Western Canada Sedimentary Basin (Western Laurussia). Geochemical proxies and MS display similar trends, suggesting an intimate interdependence. The data is thus evaluated within 1) a regional sequence stratigraphic perspective and 2) the marine-terrestrial teleconnections model (Algeo & Sheckler, 1998), whereby the rise and expansion of arborescent vascular land plants (the first 'true' forests) results in a transient increase in pedogenesis and solute delivery (hence biolimiting micronutrients) to the oceans. The *punctata* Event approximately coincides temporally with the advent of archaeopterid forest expansion and rise to dominance in the Frasnian-Fammenian age. This evolutionary event is speculated to have amplified the detrital influx which was likely already elevated by conditions of sea level lowstand, early transgression, episodes of mountain building and increased weathering during Frasnian warming. Statistical correlations among proxies suggest that changes in detrital input were the main driver of a bioproductivity increase. Elevated organic matter export from the photic zone likely led to the deposition and later preservation of organic-carbon rich facies under facilitated conditions of bottom water oxygen depletion. This paper is intended to supplement the growing body of work aimed at elucidating the causes of the *punctata* Event and documenting ecosystem responses to major perturbations of the global carbon cycle.

**KEYWORDS**: *punctata* Event, geochemistry, trace element proxies, magnetic susceptibility, archaeopterid forests

## 1. Introduction

In this contribution we report changes in the geochemistry (major (>1%), minor (<1%) and trace (ppm) elements), magnetic susceptibility (MS) and total organic carbon (TOC) recorded in the basinal limestones of the Miette carbonate platform during the early Late Devonian *punctata* Event (early Middle Frasnian (E-MF) transition) in the Western Canada Sedimentary Basin. This event, occuring within and named after the *Palmatolepis punctata* conodont biostratigraphic zone, is characterized by one of the larger positive carbon isotope ($\delta^{13}C$) excursions know to date in the Phanerozoic (a shift of up to ~6-7 ‰ in the $\delta^{13}C$ reservoir (Yans et al., 2007), although more commonly reported as 4-5‰, occurring in four distinct steps described by Racki et al., 2004; Pisarzowska et al., 2006; Pisarzowska, 2008). It has been recognized as a global perturbation (or reorganization) of the carbon cycle (Yans et al., 2007; Racki et al., 2008) and its particular geochemical signatures have been found in multiple localities around the world - most notably in Belgium (Yans et al., 2007; Da Silva et al., this volume), the Holy Cross Mountains of Poland (Racki et al., 2004; Pisarzowska et al., 2006; Pisarzowska, 2008), South and Central-West China (Ma et al., 2008), Nevada in the western USA (Morrow et al., 2009), and also in the Western Canada Sedimentary Basin (Holmden et al., 2006). The triggering mechanism(s) that caused this event are not yet satisfactorily explained. Racki et al. (2008, p. 127) observed that no major sea level change nor any primary climatic or evolutionary turning point is associated with this large-scale perturbation. However, Da Silva et al. (this volume) identified severe and rapid sea level changes associated with the *punctata* Event. While the *punctata* Event does not culminate in a major extinction episode, it could be argued that the rapid and unprecedented evolution and expansion of archaeopterid forests in the mid-Frasnian could be viewed as a evolutionary turning point (Kasig & Wilder, 1983; Wilder, 1994; Algeo & Sheckler, 1998). Algeo & Scheckler's (1998) terrestrial-marine teleconnections model provides an intricate

contextual framework for understanding the major ecosystem adjustments of the Devonian. Close temporal associations exists between Late Devonian marine anoxic events, pulses of extinction, major excursions in various geochemical records and paleobotanical developments in the terrestrial realm (Algeo et al., 1995; Racki, 2005). The rise of vascular plants and the resulting impact to the Devonian global ecosystem has also been assayed by Wright (1990), Berner (1997, 1998), Scheckler (2001), Beerling & Berner (2005), and an attempt to quantify the effect of vascular plants on weathering has been reported by Moulton & Berner (1998) for a field study in Iceland. The strength, timing, setting and causes of various mid-Palaeozoic extinctions associated with the many geochemical disturbances observed in this time period were reviewed by House (2002). Twenty 'short-term' events were recognized, each characterized by a distinctive 'brief' sedimentary and/or faunal perturbation (an interesting discussion on the meaning of 'abruptness' with increasing age in the geological record was discussed by van Loon, 1999).

The Late Devonian was a period of rapid and major changes in the biospheres of both the terrestrial and marine realms (Algeo et al., 1995; Algeo & Scheckler, 1998; House, 2002; Streel et al., 2000; Racki, 2005; Joachimski et al., 2009). The *punctata* Event may represent a pulse of change in response to terrestrial afforestation, superimposed on the 'extensive adjustments' which were taking place within the Devonian ecosystem, among them the progressive colonization of terrestrial habitats by both metazoans and plants, a shift from greenhouse to icehouse climatic conditions together with pulses of Eovariscan and Ellesmerian orogenic activity (Caputo, 1985; Tait et al., 1997; Savoy et al., 2000; Stevenson et al., 2000; Streel et al. 2000; Matte, 2001; Echarfaoui et al. 2002; Tribovillard et al., 2004; Caputo et al., 2008; Racki et al., 2008; Joachimski et al., 2009; Elrick et al., 2009). The current state of research on this global geochemical perturbation (Yans et al., 2007) and the associated biotic response is brought together in a collection of publications edited by Baliński et al. (2006) and Racki et al. (2008). These include studies of $\delta^{13}C$ variations, seawater $^{87}Sr/^{86}Sr$ trends, magnetic susceptibility (MS), and trace element variations as tracers of oceanic bioproductivity and paleoredox conditions. Of all the geochemical records compiled thus far, however, only the carbon isotope excursions are documented globally. The geographic extent of supporting geochemical studies is not yet sufficient nor comprehensive enough to cross-compare records from the various localities where the *punctata* Event $\delta^{13}C$ excursion has been recognized. Most of these, thus far, have focused on the stratigraphic sections of the Holy Cross Mountains (Poland) (John et al., 2008; Marynowski et al., 2008; Nawrocki et al., 2008). A common problem of Late Devonian (bio)geochemical studies is a lack of refined trends at the inter-basinal scale (Racki, 2005). Thus here we present supporting data from the distant Western Canada Sedimentary Basin. Supporting trace element trends for the *punctata* interval have been published for a stratigraphic section in the South China Basin, but hydrothermal overprinting of those geochemical signatures severely complicates their interpretation (Ma et al., 2008). The trace element data presented here is believed to represent a near-primary record across the E-MF, and will contribute to the existing body of work on this 'brief' time period (0.5-1.0 Ma) of pronounced but poorly understood change.

## 2. Geological background

For this study we examined a portion of the Miette carbonate platform margin stratigraphic profile (Section AB, Whalen & Day, 2008) containing the *Palmatolepis punctata* conodont biozone and portions of the underlying *P.transitans* and overlying *P.hassi* zones, encompassing

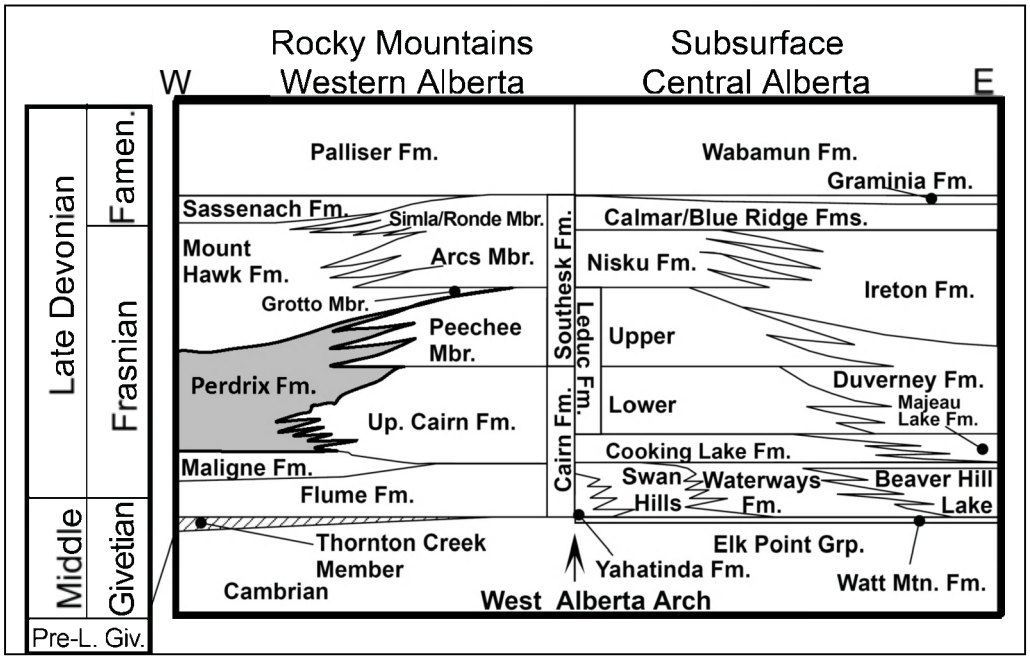


**Figure 1**. Schematic stratigraphy for the Upper Devonian of the Rocky Mountains of Western Alberta and the central Alberta subsurface, for which an independent stratigraphic nomenclature was developed (figure modified from Whalen et al., 2000).

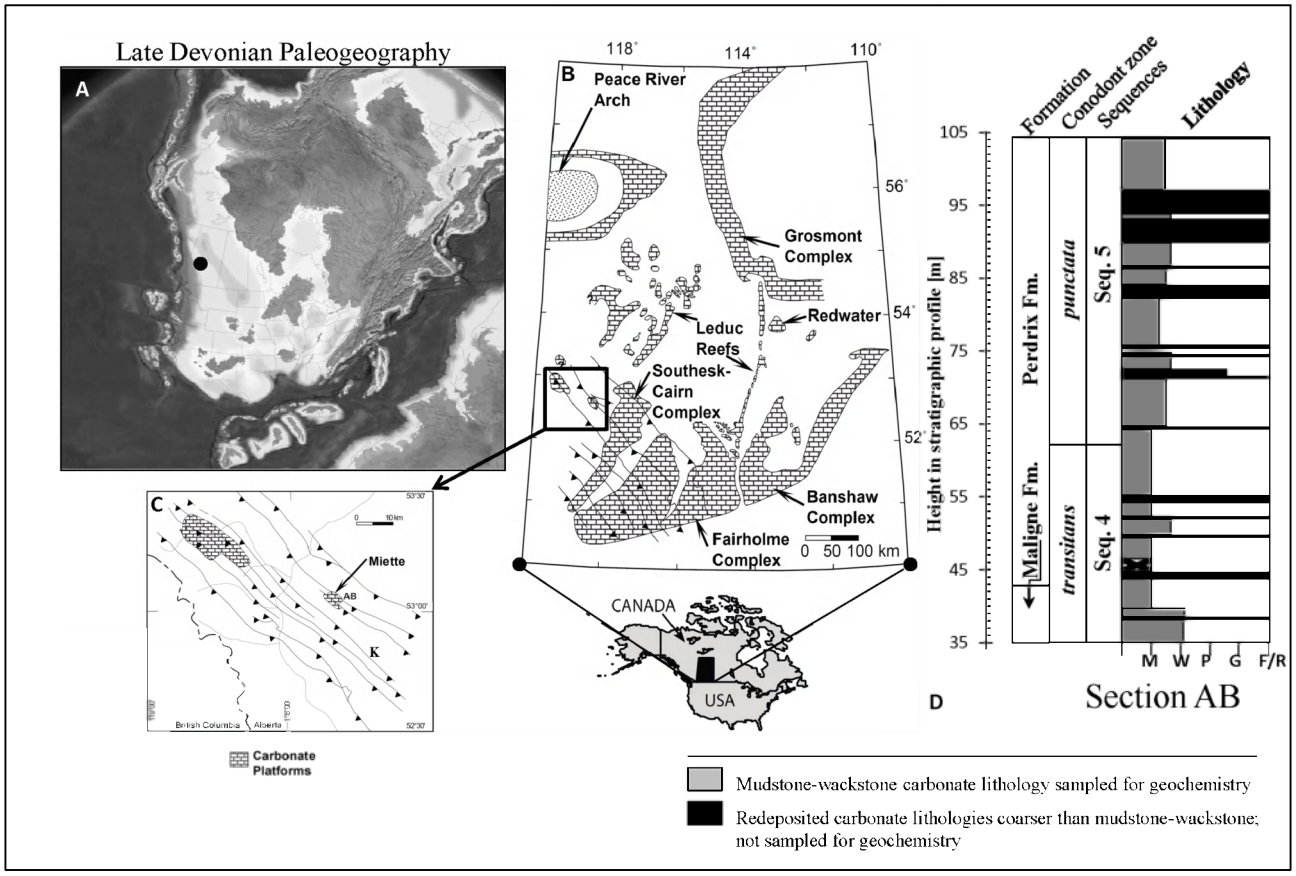


**Figure 2**. A. Paleogeographic reconstruction of Ron Blakey (http://jan.ucc.nau.edu/~rcb7/globaltext2.html, Northern Arizona University, Geology) of Late Devonian North America. Black dot indicates the paleolocality of the study area. B. Location of the Miette carbonate platform within the greater Western Canada Sedimentary Basin. C. Location of the Miette platform within the thrust belts of Western Alberta. 'AB' denotes the location of stratigraphic Section AB investigated in this study. 'K' denotes the location of Section K, a correlatable section in an adjacent thrust sheet. (Insets B and C modified from Whalen et al., 2000). D. Generalized lithostratigraphic profile for Section AB.

the topmost Maligne and lower Perdrix formations (Fig. 1). This platform is located in the Western Canada Sedimentary Basin, which, during the Late Devonian, was situated at near-equatorial latitudes on the western coast of the Laurussian continent (Fig. 2). With an areal extent of ~165 km$^2$ and a thickness of 400-500 m (Geldsetzer, 1989; Mountjoy, 1989), it was one of a system of attached and isolated platforms that developed during the Frasnian age atop a preexisting carbonate ramp which had formed across an extensive subaerial unconformity during the Middle and Late Devonian transgressions. Platform growth kept pace with a 2$^{nd}$ order sea level rise (Fig. 3) and rates of platform sedimentation surpassed those of the associated basins (Whalen et al., 2000). These basins are filled with platform-derived carbonate material variably mixed with fine-grained siliciclastic sediment, likely of Ellesmerian Fold Belt (Canadian Arctic Archipelago) or continental Laurussian provenance (Oliver & Cowper 1963; Stoakes, 1980; Switzer et al., 1994; Whalen & Day, 2008). Extensive reef development ceased in this region following the Frasnian-Fammenian mass extinction event which exterminated the stromatoporoid-coral frame-building fauna (McLaren, 1982; McLaren & Goodfellow, 1990; Stearn, 1987). The development of the Miette platform was subdivided into four phases, detailed in Whalen et al. (2000). A current total of nine 3$^{rd}$ order sea level change depositional sequences characterize these four phases which span the Late Givetian to Early Fammenian (Whalen & Day, 2008). Strata containing evidence of the *punctata* Event are situated across and just above the boundary of Sequences 4 & 5 of Whalen & Day (2008), which was a time period of rimmed platform progradation (Seq. 4) followed by backstepping and aggradation of a relatively flat-topped, isolated platform with a bypass margin (Seq. 5 & 6) (Whalen et al., 2000).

The biostratigraphy and sequence stratigraphy for the Section AB profile was established within the context of recent work by Whalen et al. (2000), Whalen & Day (2008) and Whalen & Day (in review). A rigorous biostratigraphy based on recovered conodonts could not be established for the upper portion of the profile because those samples did not yield sufficient fossils. The biostratigraphy is reinforced based on correlations with an equivalent section in an adjacent thrust sheet (Section K), for which firm biostratigraphic constraints have been established (Whalen & Day, 2008, p. 304). Variations and correlations of the magnetic susceptibility (MS) signature

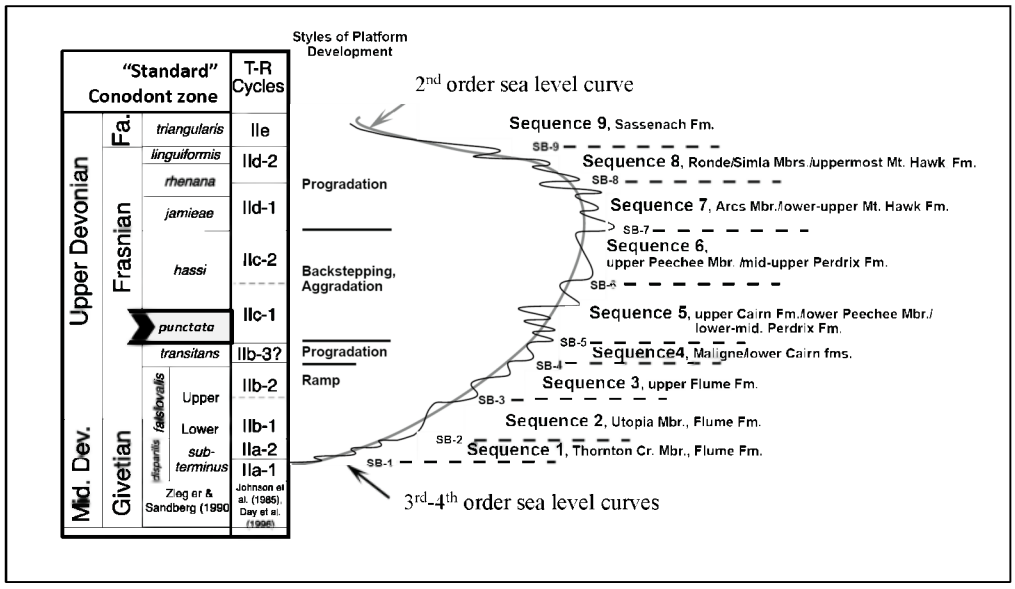


**Figure 3**. Sequence stratigraphy, conodont zonations and interpreted sea level curve developed for the study area. Figure modified from Whalen et al., (2000). The geochemical perturbation of the *punctata* Event coincides with the late sea level highstand of Sequence 4, lowstand at the boundary between Sequences 4 and 5 and with early transgressive pulse IIc1 of Sequence 5, during a period of carbonate platform backstepping and aggradation.

of Section AB and other stratigraphic profiles in the study area were used to establish its sequence stratigraphy and to further reinforce the sparse biostratigraphic constraints (Whalen & Day, 2008; Whalen & Day, in review).

The sampled interval (67 m; Fig. 2) encompasses the topmost portion of *P.transitans* conodont biozone (upper Montagne Noire Zone 4 of Klapper, 1989) and most of the *P.punctata* zone (Montagne Noire Zones 5 and 6 of Klapper, 1989). The exact stratigraphic position of the *P. punctata* and overlying *P.hassi* zonal boundary (above the observed trace element excursions – Sec. 4) could not, however, be precisely located. MS and biostratigraphic correlations with adjacent sections suggest it is situated within a 28 m covered interval which sits almost 20 m above the sampled horizons. According to the recalibrated Devonian time scale of Kaufmann (2006), conodont zonal resolution averages 0.6 Ma in the highly resolved part of the time scale (mid-Eifelian to the Devonian-Carboniferous boundary). The *punctata* Event may thus be limited to a time period of less than 600 k.y. (taken together, all 57 Devonian conodont zones give an average duration of about 1 Ma).

The stratigraphic profile consists of stark alternations of organic-rich carbonate mudstones and coarser carbonate lithologies redeposited from upslope, mostly floatstones and rudstones. Some basinal facies horizons within the region are bioturbated, while others lack benthic fauna, are laminated and contain framboidal pyrite, indicating changes from oxygenated to oxygen-depleted bottom water conditions (Whalen et al., 2000). Detailed facies descriptions of the Miette carbonate platform were previously reported by Whalen et al. (2000) and facies descriptions of the broader Western Canada Sedimentary Basin have been provided by Klovan (1964), Stoakes (1980) and van Buchem et al. (1996), among others. Stoakes (1980) reports that the chief minerals present in the basin filling facies are calcite, dolomite, illite and fine-grained quartz. This is consistent with our unpublished observations of x-ray diffraction patterns of Section AB lithologies. Only the mudstones-wackstones were sampled (n = 43) for analyses so as to avoid any potential biases associated with facies redeposited from up-slope.

## 3. Methods

### *3.1 Geochemical proxies from XRF, TOC, and MS analyses*

Minor and trace element abundances in the rock record provide insight into prevailing oceanic paleobioproductivity (Ni, Cu, P, Ba, Zn), indicate changes in the relative influx of terrigenous siliciclastic material into depositional basins (Al, Si, Ti, K, Cr, Zr, Co), and record the redox conditions near the sediment-water interface (U, Mo, V) (Calvert & Pedersen, 1993; Tribovillard et al., 2006; Algeo & Maynard, 2008; Piper & Calvert, 2009). Various other elements were previously measured and different ratios employed to further interpret conditions in the depositional environment. For example, redox-sensitive trace element ratios (Ni/Co, U/Th, V/Cr, V/(V+Ni)) were used by various authors (e.g. Hatch & Leventhal, 1992; Jones & Manning, 1994; Rimmer, 2004; Rimmer et al., 2004; Riquier et al., 2006; Algeo & Maynard, 2008) as indicators of bottom water oxygen levels. Riquier et al. (2006) additionally measured Mn to further infer whether the boundary between oxidizing and reducing conditions resided within the water column or near the sediment-water interface. Pb, Fe, Zn and the Fe/S ratio were applied as proxies for pyrite, hence as supplementary indicators of sulfate reducing conditions (Riquier et al., 2006). A Fe-S crossplot with a slope of 1.15 – that of stoichiometric pyrite – assumes all Fe is secured as this sulfide (Riquier et al., 2006; Rimmer, 2004). Ratios of detrital proxy elements were also evaluated and interpreted in terms of changes in relative sedimentation rates (Ti/Al – Bertrand et al., 1996; Murphy et al., 2000; Zr/Al – Piper & Calvert, 2009).

It is common practice to normalize trace element abundances in marine sedimentary rocks (especially

shales) to the Al content as a means of decoupling the detrital trace element contribution from the overall signal (Calvert & Pedersen, 1993; van der Weijden, 2002; Rimmer, 2004; Rimmer et al., 2004; Riquier et al., 2006; Ma et al. 2008). Al is cited as being 'overwhelmingly of detrital origin' (Riquier et al., 2006; Tribovillard et al., 2006). More intricate ways of manipulating and presenting trace element data are discussed by Algeo & Maynard (2008). It seems questionable whether this practice, as applied to shales, is equally applicable to carbonate lithologies. The seawater trace element signal recorded in a shale lithology is severely masked behind the stronger signal of trace element concentrations in the siliciclastic fraction of the rock. Shales also contain variable amounts of opal and carbonate, both of which act as 'dilutants' of the authigenic trace element signature. This necessitates a 'signal decoupling procedure' such as Al-normalization. The mechanism of trace element enrichment is however different for carbonate lithologies. Minor (Mg, Sr) and trace elements (commonly Cd, Mn, Fe, Co, Zn, Ni, Pb, Ba, Eu, K) are incorporated via 1) substitution for the $Ca^{2+}$ cation in the $CaCO_3$ crystal structure, 2) inclusion between crystallographic planes, 3) incorporation into defected, empty lattice positions and 4) via surface adsorption (Veizer, 1983). They also reside within a limestone's siliciclastic fraction.

Such methods of data manipulation as Al-normalization and enrichment factor calculations were critically evaluated by van der Weijden (2002) with surprising results. Using Al (or another element) as a common divisor, uncorrelated variables can acquire false correlations. Preexisting interrelationships between variables may be enhanced, distorted, changed from positive to negative (and vice versa) or may be destroyed altogether. This is especially so if the coefficient of variance of the devisor (standard deviation divided by the mean) is high. Theses effects are minimized or do not occur altogether when the coefficient of variance is small. But if such is the case, a normalization procedure is unnecessary altogether (van der Weijden, 2002).We thus present an unmodified trace element dataset for a suite of samples consisting of a near-constant carbonate mudstone lithology.

The major, minor and trace element data was generated using a PANalytical Axios wavelength-dispersive x-ray fluorescence spectrometer (XRF) at the University of Alaska Fairbanks Advanced Instrumentation Laboratory. A custom pressed-pellet trace element analytical routine specific to this particular carbonate lithology was developed. A major focus of routine development was to be able to detect single digit concentrations of certain trace elements and to obtain an analytical resolution capable of distinguishing concentration differences across samples down to 1 ppm (parts per million). The routine quantifies Al, Si, P, S, K, Ti, V, Cr, Mn, Fe, Co, Ni, Cu, Zn, Sr, Zr, Mo, Ba, U, Th, Rb and Pb in a dominantly carbonate matrix. Each analyte was calibrated against 'in-house' and certified standard reference materials (available from the United States Geological Survey and the United States National Institute of Standards and Technology). The analytical accuracy based on calibrations relative to standard reference materials is within 10%. The reproducibility of results is to within several tens of parts per million for those elements present in concentrations of several hundred to several thousand ppm, and is around one-tenth of a ppm for those elements generally present in concentrations below 100 ppm. Calculated lowest levels of detection for each analyte along with representative analytical precisions are summarized in Table 1.

Samples were pulverized using hardened steel vials from SPEX CertiPrep Group. Because of the relative softness of the lithology, a 5 minute crushing time was sufficient to produce a homogenous powder. Each sample was subsequently made into a 35 mm diameter pressed pellet using polyvinyl alcohol as a binder.

| **Element** | **Al** | **Si** | **P** | **S** | **Ti** | **V** | **Cr** | **Mn** | **Fe** | **Co** |
|---|---|---|---|---|---|---|---|---|---|---|
| Analyte measured in units of: | (%) | (%) | (%) | (%) | (ppm) | (ppm) | (ppm) | (ppm) | (ppm) | (ppm) |
| Lowest level of detection (LLD) for typical analysis of this lithology [ppm] | N/A because analyte is measured in wt.% | | | | 1.4 | 0.6 | 1.4 | 1.7 | 2.3 | 0.3 |
| Representative analytical precision [ppm] | 4.1 | 33.4 | 0.0 | 0.0 | 0.6 | 0.2 | 0.1 | 0.8 | 0.2 | 0.2 |
| **Element** | **Ni** | **Cu** | **Zn** | **Sr** | **Zr** | **Mo** | **Ba** | **K** | **Rb** | **Pb** |
| Analyte measured in units of: | (ppm) | (ppm) | (ppm) | (ppm) | (ppm) | (ppm) | (ppm) | (ppm) | (ppm) | (ppm) |
| Lowest level of detection (LLD) for typical analysis of this lithology [ppm] | 0.7 | 0.7 | 0.6 | 0.6 | 0.5 | 0.3 | 4.7 | 3.7 | 0.2 | 0.2 |
| Representative analytical precision [ppm] | 0.1 | 0.4 | 0.2 | 1.0 | 0.3 | 0.1 | 1.1 | 0.0 | 0.0 | 0.1 |
| **Element** | **Th** | **U** | | | | | | | | |
| Analyte measured in units of: | (ppm) | (ppm) | | | | | | | | |
| Lowest level of detection (LLD) for typical analysis of this lithology [ppm] | 0.1 | 0.2 | | | | | | | | |
| Representative analytical precision [ppm] | 0.4 | 0.0 | | | | | | | | |

**Table 1**. Lowest levels of detection and representative analytical precisions for each minor and trace element analyzed based on calibrations of the custom x-ray fluorescence (XRF) analytical routine developed for this study.

### *3.2 Total Organic Carbon (TOC) determination*

TOC was determined using a ECS 4010 Elemental Combustion System at the Alaska Stable Isotope Facility (University of Alaska Fairbanks) during $\delta^{13}C_{org}$, $\delta^{13}C_{carb}$, $\delta^{18}O_{carb}$ and $\delta^{15}N_{org}$ data generation (not reported here). TOC concentrations present in the acid-insoluble residue following carbonate acidification were used to calculate the TOC for the bulk rock based on the initial mass measured before processing. The analytical precision and accuracy associated with the TOC analysis is within 2% and 10% of the reported values.

### *3.3 Magnetic susceptibility determinations*

Samples for magnetic susceptibility measurements were weighed to within 0.001 g and measured on a KLY-3 Kappa bridge magnetic-susceptibility meter at Brooks Ellwood's lab (Louisiana State University). MS values represent an average of three measurements of mass-normalized bulk magnetic susceptibility (with units of $m^3/kg$), taken on each sample. Previous work by Whalen & Day (2008) indicates that the MS is dominated by the paramagnetic component.

## 4. Results

Prominent trace element variations are observed within the *P.punctata* conodont biozone and correspond to the large, globally distributed, $\delta^{13}C$ excursion (Racki, 2004, 2005; Holmden et al., 2006; Pisarzowska et al., 2006; Yans et al., 2007; Ma et al., 2008; Racki et al., 2008; Morrow et al., 2009). Geochemical proxies for changes in detrital input (Fig. 4), bioproductivity (Fig. 6), oceanic paleoredox conditions (Fig. 6) and MS (Figs 4 & 5) during the *punctata* Event display similar trends, indicating that these proxies and MS are inherently linked. The stratigraphic distribution of proxies reveals a first-order enrichment in the 50-75 m interval of the profile, which can be subdivided into two excursions (at around 64 m and 72.5 m in profile) separated by a trough (at around 65-70 m in profile) where trace element values return to 'background' levels. Both excursions are generally characterized by at least a two-fold increase in trace element concentrations above stratigraphic background, and bulk-rock TOC is elevated from an average of 0.2 (wt.%) to 2.5 (wt.%) and 1.0 (wt.%) during the lower and higher peaks, respectively (Fig. 6).

Correlation coefficients (Person's r and Spearman's rho) (Davis, 2002) were calculated among the elements (Tables 3 & 4), and significant correlations were found to exist (the raw geochemical dataset is in Appendix A). The observed interdependence between bioproductivity and detrital input proxies and MS implies that primary production increases during the *punctata* Event were driven largely by changes in detrital supply and associated nutrients. Similar overall trends in, and correlations between, paleoredox proxies and TOC (Fig. 6, Tables 3 & 4) suggest that low bottom water oxygen conditions were responsible for the preservation of organic matter (OM) produced during detrital-driven high productivity. Evaluation of the data from a sequence stratigraphic perspective implies that trends are likely influenced by relative sea level change. Most proxies display an initial

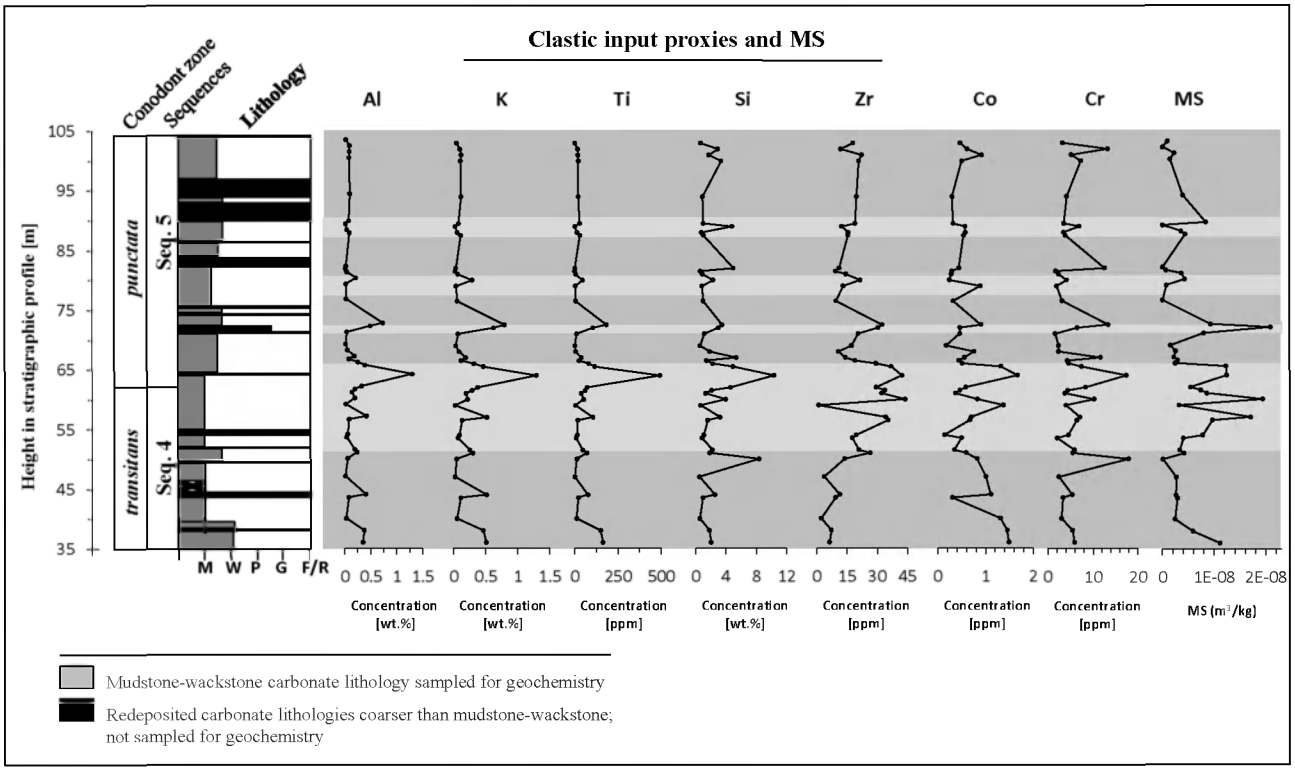


**Figure 4**. Chemostratigraphic profiles of elements used as proxies for terrigenous clastic influxes into marine depositional basins. Plotted also is the corresponding magnetic susceptibility (MS) profile. Shaded areas are meant to help visualize common trends.

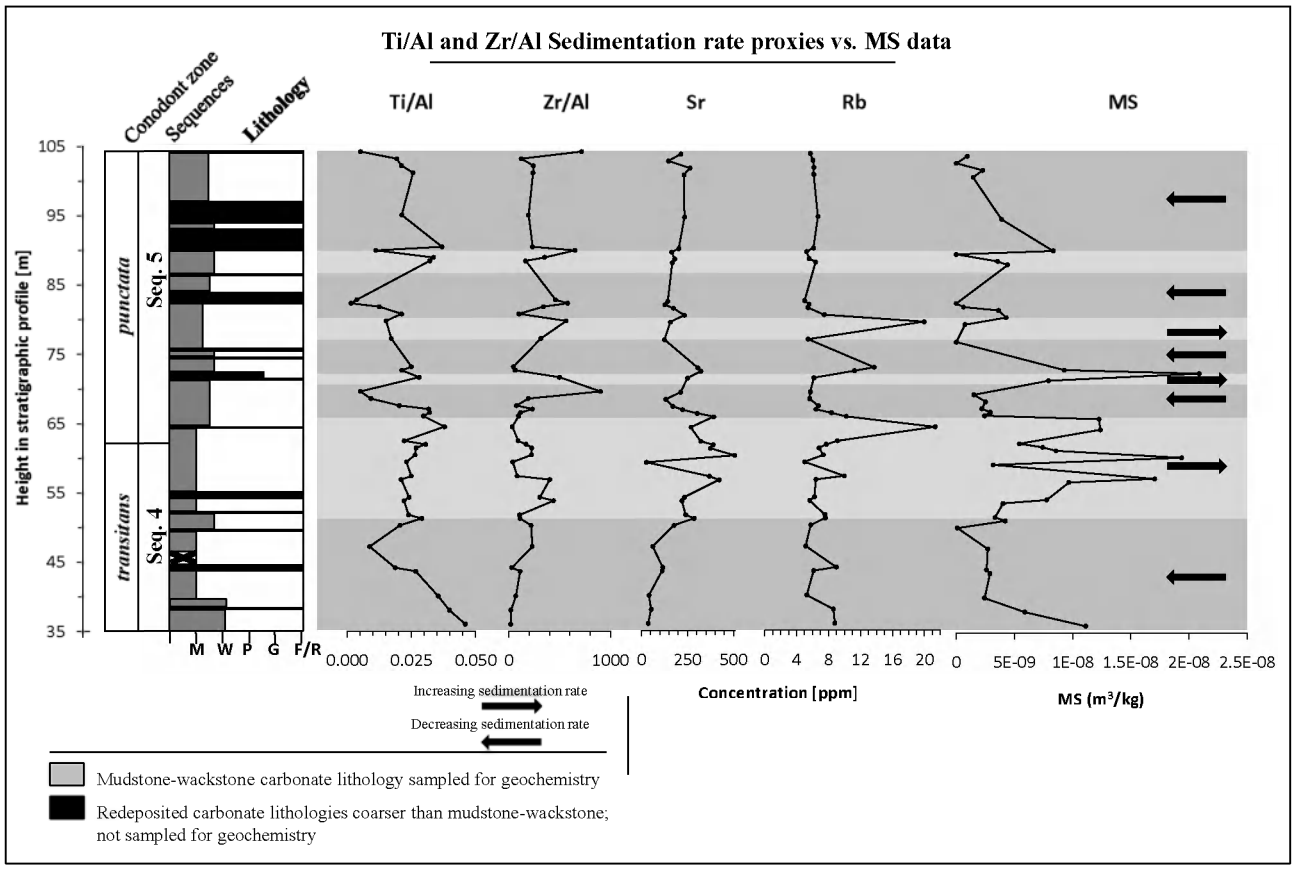


**Figure 5**. The Ti/Al and Zr/Al ratios plotted against the magnetic susceptibility (MS) profile for stratigraphic Section AB. Plotted also are the quasi-proxies for continental weathering – Rb & Sr. Shaded areas are meant to help visualize common trends.

increase during 3rd order sea level lowstand and early transgression (transition between Sequences 4-5), and eventually return to 'background' levels during sea level highstand.

Following the approach of Bertrand et al. (1996) and Piper & Calvert (2009), the Ti/Al and Zr/Al ratios were employed as proxies for changes in relative sedimentation rates and plotted against both MS and the speculative quasi-proxies for continental weathering – Rb and Sr (Fig. 5). Increasing Ti/Al and Zr/Al ratios of marine sediments correlate with increasing grain size of mud-dominated facies. This observation was used by Murphy et al. (2000)

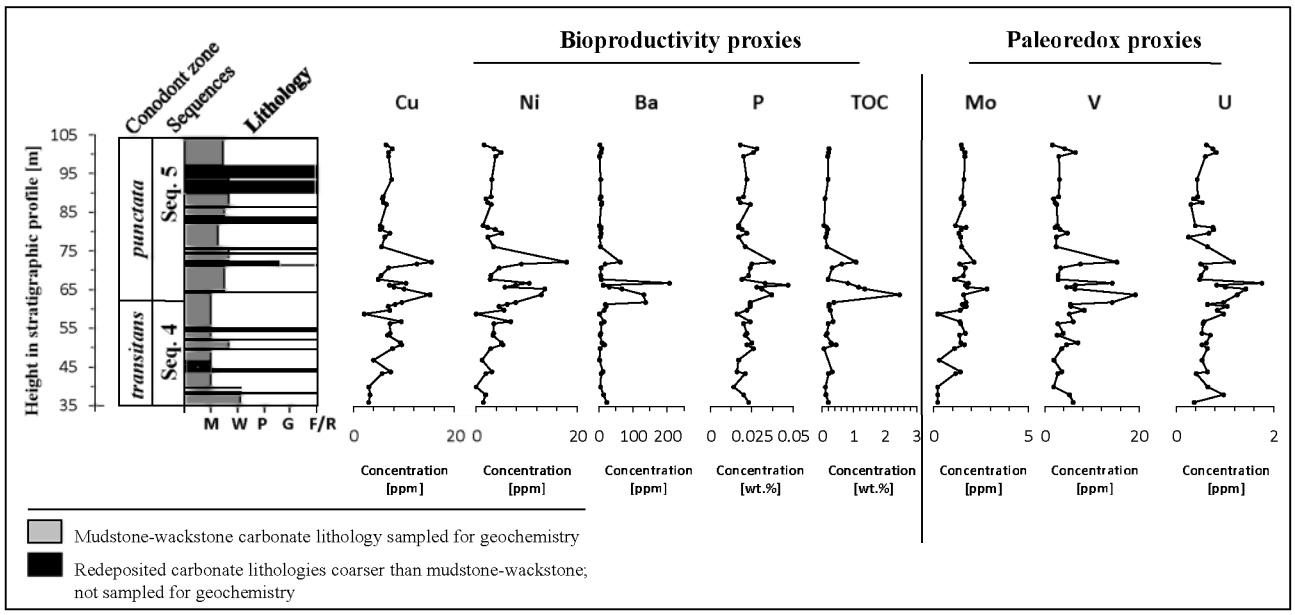


**Figure 6**. Chemostratigraphic profiles of bioproductivity and paleoredox proxies and the stratigraphic distribution of total organic carbon (TOC).

**Person's r Correlations**

| | MS | Al | Si | K | Ti | Zr | Cr | Ni | Cu | Ba | P | TOC | Mo | V | U | Fe | S | Ph | Zn | Mn | Co | Th | Sr | Rb |
|---|---|---|---|---|---|---|---|---|---|---|---|---|---|---|---|---|---|---|---|---|---|---|---|---|
| MS | 1.000 | .533** | .166 | .580** | .474** | .697** | .138 | .474** | .431** | .149 | .338* | .363* | .091 | .412* | .161 | .425* | .374* | .285 | -.218 | .213 | .252 | .015 | .628** | .356* |
| Al | .533** | 1.000 | .582** | .990** | .965** | .523** | .511** | .713** | .725** | .518** | .665** | .839** | .138 | .795** | .450** | .922** | .797** | .819** | -.077 | .609** | .571** | -.213 | .235 | .739** |
| Si | .166 | .582** | 1.000 | .517** | .584** | .352* | .882** | .480** | .542** | .552** | .548** | .600** | .185 | .613** | .414* | .623** | .648** | .536** | .350* | .379* | .398* | -.211 | .181 | .383* |
| K | .580** | .990** | .517** | 1.000 | .946** | .519** | .449** | .695** | .693** | .478** | .632** | .795** | .104 | .760** | .413* | .902** | .749** | .803** | -.118 | .611** | .573** | -.214 | .242 | .719** |
| Ti | .474** | .965** | .584** | .946** | 1.000 | .450** | .488** | .592** | .590** | .485** | .619** | .834** | .026 | .738** | .413* | .943** | .837** | .778** | -.092 | .739** | .638** | -.350* | .144 | .729** |
| Zr | .697** | .523** | .352* | .519** | .450** | 1.000 | .294 | .671** | .694** | .294 | .550** | .554** | .566** | .533** | .371* | .404* | .541** | .341* | -.211 | .002 | .046 | .417* | .946** | .396* |
| Cr | .138 | .511** | .882** | .449** | .488** | .294 | 1.000 | .464** | .544** | .457** | .603** | .466** | .124 | .596** | .384* | .512** | .448** | .488** | .387* | .253 | .343* | -.220 | .156 | .288 |
| Ni | .474** | .713** | .480** | .695** | .592** | .671** | .464** | 1.000 | .895** | .652** | .863** | .778** | .647** | .809** | .701** | .616** | .635** | .607** | .157 | .197 | .210 | .262 | .528** | .528** |
| Cu | .431** | .725** | .542** | .693** | .590** | .694** | .544** | .895** | 1.000 | .556** | .804** | .743** | .618** | .767** | .490** | .566** | .611** | .581** | .112 | .044 | .065 | .329 | .546** | .571** |
| Ba | .149 | .518** | .552** | .478** | .485** | .294 | .457** | .652** | .556** | 1.000 | .640** | .633** | .329 | .836** | .779** | .538** | .567** | .546** | .555** | .366* | .251 | .009 | .155 | .368* |
| P | .338* | .665** | .548** | .632** | .619** | .550** | .603** | .863** | .804** | .640** | 1.000 | .768** | .503** | .796** | .705** | .610** | .645** | .587** | .299 | .331 | .224 | .082 | .390* | .442** |
| TOC | .363* | .839** | .600** | .795** | .834** | .554** | .466** | .778** | .743** | .633** | .768** | 1.000 | .438** | .734** | .638** | .874** | .942** | .802** | .071 | .596** | .442** | -.017 | .300 | .657** |
| Mo | .091 | .138 | .185 | .104 | .026 | .566** | .124 | .647** | .618** | .329 | .503** | .438** | 1.000 | .290 | .456** | .077 | .360* | .210 | -.008 | -.310 | -.308 | .788** | .595** | .162 |
| V | .412* | .795** | .613** | .760** | .738** | .533** | .596** | .809** | .767** | .836** | .796** | .734** | .290 | 1.000 | .686** | .694** | .643** | .628** | .267 | .385* | .353* | -.038 | .330 | .573** |
| U | .161 | .450** | .414* | .413* | .413* | .371* | .384* | .701** | .490** | .779** | .705** | .638** | .456** | .686** | 1.000 | .529** | .573** | .564** | .503** | .346* | .271 | .026 | .269 | .197 |
| Fe | .425* | .922** | .623** | .902** | .943** | .404* | .512** | .616** | .566** | .538** | .610** | .874** | .077 | .694** | .529** | 1.000 | .889** | .862** | .038 | .799** | .717** | -.378* | .114 | .672** |
| S | .374* | .797** | .648** | .749** | .837** | .541** | .448** | .635** | .611** | .567** | .645** | .942** | .360* | .643** | .573** | .889** | 1.000 | .750** | .024 | .651** | .502** | -.096 | .290 | .626** |
| Pb | .285 | .819** | .536** | .803** | .778** | .341* | .488** | .607** | .581** | .546** | .587** | .802** | .210 | .628** | .564** | .862** | .750** | 1.000 | .132 | .609** | .580** | -.172 | .099 | .523** |
| Zn | -.218 | -.077 | .350* | -.118 | -.092 | -.211 | .387* | .157 | .112 | .555** | .299 | .071 | -.008 | .267 | .503** | .038 | .024 | .132 | 1.000 | .050 | .051 | -.223 | -.191 | -.134 |
| Mn | .213 | .609** | .379* | .611** | .739** | .002 | .253 | .197 | .044 | .366* | .331 | .596** | -.310 | .385* | .346* | .799** | .651** | .609** | .050 | 1.000 | .800** | -.699* | -.249 | .432** |
| Co | .252 | .571** | .398* | .573** | .638** | .046 | .343* | .210 | .065 | .251 | .224 | .442** | -.308 | .353* | .271 | .717** | .502** | .580** | .051 | .800** | 1.000 | -.671* | -.157 | .503** |
| Th | .015 | -.213 | -.211 | -.214 | -.350* | .417* | -.220 | .262 | .329 | .009 | .082 | -.017 | .788** | -.038 | .026 | -.378* | -.096 | -.172 | -.223 | -.699* | -.671* | 1.000 | .563** | -.092 |
| Sr | .628** | .235 | .181 | .242 | .144 | .946** | .156 | .528** | .546** | .155 | .390* | .300 | .595** | .330 | .269 | .114 | .290 | .099 | -.191 | -.249 | -.157 | .563** | 1.000 | .166 |
| Rb | .356* | .739** | .383* | .719** | .729** | .396* | .288 | .528** | .571** | .368* | .442** | .657** | .162 | .573** | .197 | .672** | .626** | .523** | -.134 | .432** | .503** | -.092 | .166 | 1.000 |

**. Correlation is significant at the 0.01 level (2-tailed).

*. Correlation is significant at the 0.05 level (2-tailed).

**Table 3**. Matrix showing Person's r correlations among the variables in the geochemical dataset (correlations calculated using the SPSS statistical software).

**Spearman's rho correlations**

| | MS | Al | Si | K | Ti | Zr | Cr | Ni | Cu | Ba | P | TOC | Mo | V | U | Fe | S | Ph | Zn | Mn | Co | Th | Sr | Rb |
|---|---|---|---|---|---|---|---|---|---|---|---|---|---|---|---|---|---|---|---|---|---|---|---|---|
| MS | 1.000 | .673** | .107 | .712** | .670** | .638** | .132 | .502** | .366* | .585** | .358* | .539** | .048 | .605** | .181 | .488** | .638** | .387* | -.161 | .134 | .198 | .327 | .608** | .637** |
| Al | .673** | 1.000 | .490** | .986** | .973** | .547** | .503** | .646** | .658** | .787** | .595** | .758** | .156 | .830** | .385* | .848** | .778** | .713** | .081 | .387* | .405* | .214 | .452** | .832** |
| Si | .107 | .490** | 1.000 | .410* | .445** | .394* | .888** | .479** | .567** | .372* | .495** | .392* | .131 | .559** | .248 | .520** | .430** | .456** | .025 | .234 | .344* | -.092 | .316 | .313 |
| K | .712** | .986** | .410* | 1.000 | .969** | .545** | .419* | .630** | .605** | .794** | .547** | .760** | .145 | .803** | .348* | .826** | .789** | .678** | .006 | .384* | .393* | .236 | .450** | .842** |
| Ti | .670** | .973** | .445** | .969** | 1.000 | .492** | .480** | .589** | .589** | .782** | .589** | .726** | .148 | .807** | .389* | .880** | .782** | .696** | .061 | .467** | .440** | .179 | .398* | .825** |
| Zr | .638** | .547** | .394* | .545** | .492** | 1.000 | .367* | .842** | .724** | .483** | .576** | .638** | .472** | .618** | .363* | .315 | .640** | .242 | -.067 | -.153 | .069 | .615** | .972** | .545** |
| Cr | .132 | .503** | .888** | .419* | .480** | .367* | 1.000 | .393* | .565** | .341* | .510** | .346* | .111 | .562** | .231 | .591** | .391* | .493** | .080 | .178 | .422* | -.086 | .297 | .303 |
| Ni | .502** | .646** | .479** | .630** | .589** | .842** | .393* | 1.000 | .849** | .667** | .759** | .827** | .611** | .767** | .559** | .433** | .751** | .414* | .200 | .053 | .049 | .504** | .789** | .588** |
| Cu | .366* | .658** | .567** | .605** | .589** | .724** | .565** | .849** | 1.000 | .579** | .746** | .758** | .529** | .683** | .363* | .515** | .711** | .532** | .176 | .111 | .088 | .501** | .673** | .622** |
| Ba | .585** | .787** | .372* | .794** | .782** | .483** | .341* | .667** | .579** | 1.000 | .619** | .836** | .416* | .792** | .544** | .683** | .805** | .691** | .006 | .508** | .323 | .308 | .448** | .712** |
| P | .358* | .595** | .495** | .547** | .589** | .576** | .510** | .759** | .746** | .619** | 1.000 | .718** | .491** | .794** | .516** | .459** | .675** | .445** | .306 | .297 | .153 | .287 | .545** | .491** |
| TOC | .539** | .758** | .392* | .760** | .726** | .638** | .346* | .827** | .758** | .836** | .718** | 1.000 | .549** | .754** | .444** | .589** | .863** | .614** | .093 | .344* | .211 | .469** | .580** | .667** |
| Mo | .048 | .156 | .131 | .145 | .148 | .472** | .111 | .611** | .529** | .416* | .491** | .549** | 1.000 | .322 | .497** | .019 | .370* | .165 | .066 | -.088 | -.183 | .643** | .489** | .219 |
| V | .605** | .830** | .559** | .803** | .807** | .618** | .562** | .767** | .683** | .792** | .794** | .754** | .322 | 1.000 | .533** | .644** | .752** | .509** | .175 | .235 | .304 | .230 | .552** | .706** |
| U | .181 | .385* | .248 | .348* | .389* | .363* | .231 | .559** | .363* | .544** | .516** | .444** | .497** | .533** | 1.000 | .374* | .474** | .393* | .388* | .252 | .211 | .143 | .315 | .227 |
| Fe | .488** | .848** | .520** | .826** | .880** | .315 | .591** | .433** | .515** | .683** | .459** | .589** | .019 | .644** | .374* | 1.000 | .698** | .788** | .206 | .613** | .574** | -.033 | .224 | .663** |
| S | .638** | .778** | .430** | .789** | .782** | .640** | .391* | .751** | .711** | .805** | .675** | .863** | .370* | .752** | .474** | .698** | 1.000 | .667** | .030 | .412* | .257 | .379* | .581** | .679** |
| Pb | .387* | .713** | .456** | .678** | .696** | .242 | .493** | .414* | .532** | .691** | .445** | .614** | .165 | .509** | .393* | .788** | .667** | 1.000 | .236 | .562** | .441** | .032 | .163 | .552** |
| Zn | -.161 | .081 | .025 | .006 | .061 | -.067 | .080 | .200 | .176 | .006 | .306 | .093 | .066 | .175 | .388* | .206 | .030 | .236 | 1.000 | .156 | .138 | -.212 | -.090 | -.063 |
| Mn | .134 | .387* | .234 | .384* | .467** | -.153 | .178 | .053 | .111 | .508** | .297 | .344* | -.088 | .235 | .252 | .613** | .412* | .562** | .156 | 1.000 | .602** | -.248 | -.197 | .356* |
| Co | .198 | .405* | .344* | .393* | .440** | .069 | .422* | .049 | .088 | .323 | .153 | .211 | -.183 | .304 | .211 | .574** | .257 | .441** | .138 | .602** | 1.000 | -.237 | -.013 | .424* |
| Th | .327 | .214 | -.092 | .236 | .179 | .615** | -.086 | .504** | .501** | .308 | .287 | .469** | .643** | .230 | .143 | -.033 | .379* | .032 | -.212 | -.248 | -.237 | 1.000 | .694** | .359* |
| Sr | .608** | .452** | .316 | .450** | .398* | .972** | .297 | .789** | .673** | .448** | .545** | .580** | .489** | .552** | .315 | .224 | .581** | .163 | -.090 | -.197 | -.013 | .694** | 1.000 | .459** |
| Rb | .637** | .832** | .313 | .842** | .825** | .545** | .303 | .588** | .622** | .712** | .491** | .667** | .219 | .706** | .227 | .663** | .679** | .552** | -.063 | .356* | .424* | .359* | .459** | 1.000 |

**. Correlation is significant at the 0.01 level (2-tailed).

*. Correlation is significant at the 0.05 level (2-tailed).

**Table 4**. Matrix showing Spearman's rho correlations among the variables in the geochemical dataset (correlations calculated using the SPSS statistical software).

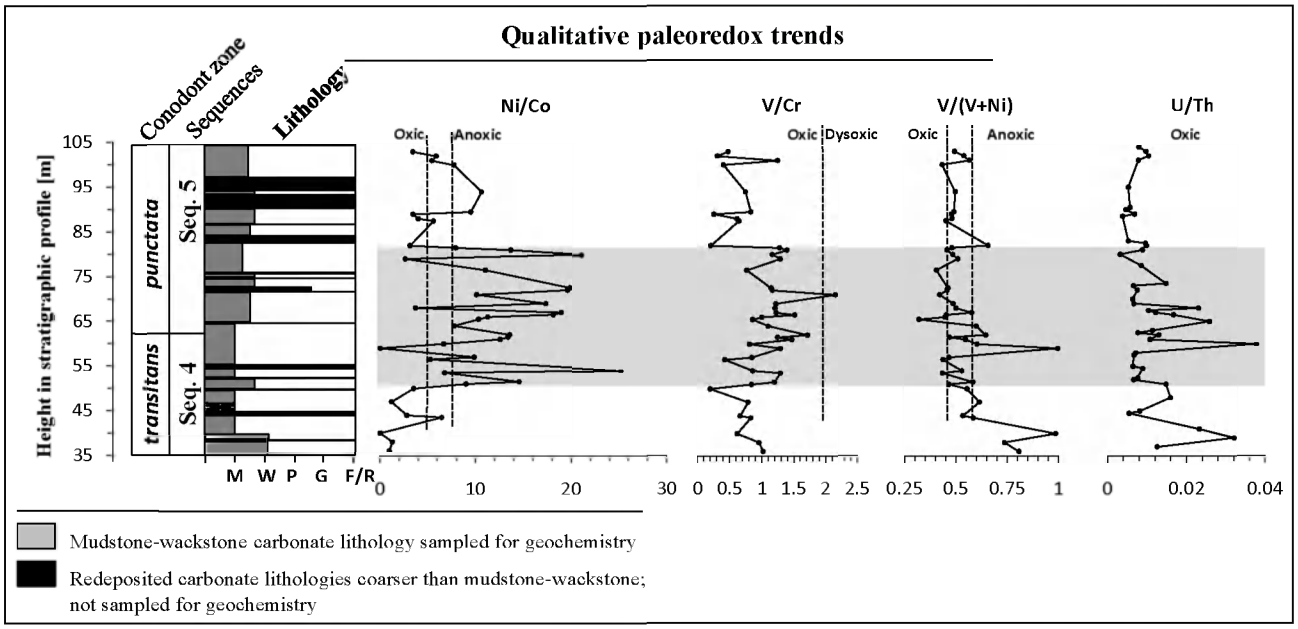


**Figure 7**. Chemostratigraphic profiles of elemental ratios used as proxies for bottom water redox conditions. Taken collectively and interpreted relatively, these indices suggest dominantly dysoxic-anoxic bottom water conditions prevailing during the *punctata* Event. Shaded area highlights the horizon of trace element enrichment.

to demonstrate changes in sedimentation rates during the deposition of Devonian black shales in the Appalachian Basin, and Piper & Calvert (2009) interpreted trends in Zr/Al values in a similar manner. Both Ti and Zr reside in the heavy mineral fraction of sediments, sequestered in rutile and zircon mineral phases, respectively. Given their high specific gravities compared to quartz (rutile: specific gravity (G) = 4.23-5.5, zircon: G=4.68, quartz: G=2.65), both minerals tend to be deposited with a coarser sand fraction (hydraulic equivalence: silt-sized zircons and rutile are approximately equivalent to sand-sized quartz) (Tucker, 2001). While both ratios follow the general trend of MS variation (corroborating hypotheses about MS and detrital input – Ellwood et al., 1999), the Zr/Al trend displays an inverse relationship, which may be an artifact of dividing Ti and Zr concentrations by Al contents (in essence a Al-normalization of the sort discussed by van der Weijden, 2002). Notice, for example, that the unnormalized Zr profile faithfully mimics the MS trend (compare Figs 4 & 5). The increases of Sr and Rb concentrations throughout the interval are observed to coincide with elevated levels of other detrital proxies and MS, possibly further supporting the notion of increased land-derived siliciclastic delivery to ocean basins. Both elements could be regarded as speculative quasi-proxies of continental weathering. John et al. (2008) observed a pulsed increase in seawater $^{87}Sr/^{86}Sr$ ratios during the onset of the *punctata* Event - an isotopic shift that should also manifest itself as a rise in the absolute concentration of Sr in seawater given that the residence time of this element in the oceans (>4 Myr) is longer than oceanic mixing rates (~$10^3$ yr) (Veizer, 1989). During fractional crystallization, both Sr and Rb are concentrated into the melt, which effectively enriches both elements in continental crust (Veizer, 1989). Uplift and increased weathering of crystalline rocks, especially in humid, warm tropical/equatorial regions will increase the flux of both elements into the oceans via riverine discharge.

| Water column oxgenation conditions: | Oxic | Dysoxic | Anoxic |
|---|---|---|---|
| Ni/Co[a] | < 5.00 | 5.00-7.00 | > 7.00 |
| V/Cr[a] | < 2.00 | 2.00-4.25 | > 4.25 |
| V/(V+Ni)[b] | < 0.46 | 0.46-0.60 | 0.54-0.82 |
| U/Th[a] | < 0.75 | 0.75-1.25 | > 1.25 |

[a] Jones and Manning (1994)

[b] Hatch and Leventhal (1992)

**Table 2**. Redox sensitive trace element ratio thresholds indicative of oxic, dysoxic and anoxic bottom water conditions (Jones & Manning, 1994; Hatch & Leventhal, (1992).

The calculated redox element ratios - Ni/Co, V/Cr, V/(V+Ni) and U/Th (Fig. 7) – were assigned the oxic-dysoxic-anoxic threshold values of Jones & Manning (1994) and Hatch & Leventhal (1992) (Table 2), although these calculations ought to be viewed only relatively (see discussion in Rimmer, 2004; see also Riquier et al., 2006). Applying a set of absolute threshold values to these ratios based either on contemporary dysoxic-anoxic basin analogues or thresholds developed for a specific paleobasin may not be appropriate for depositional environments of a different age, a different paleogeographic setting, or supplied with detritus of a different provenance. These redox indices are suggested to be used collectively to interpret the degree of anoxia based on relative variations (Rimmer, 2004). Absolute thresholds established in previous studies ought not to be applied strictly (Rimmer,

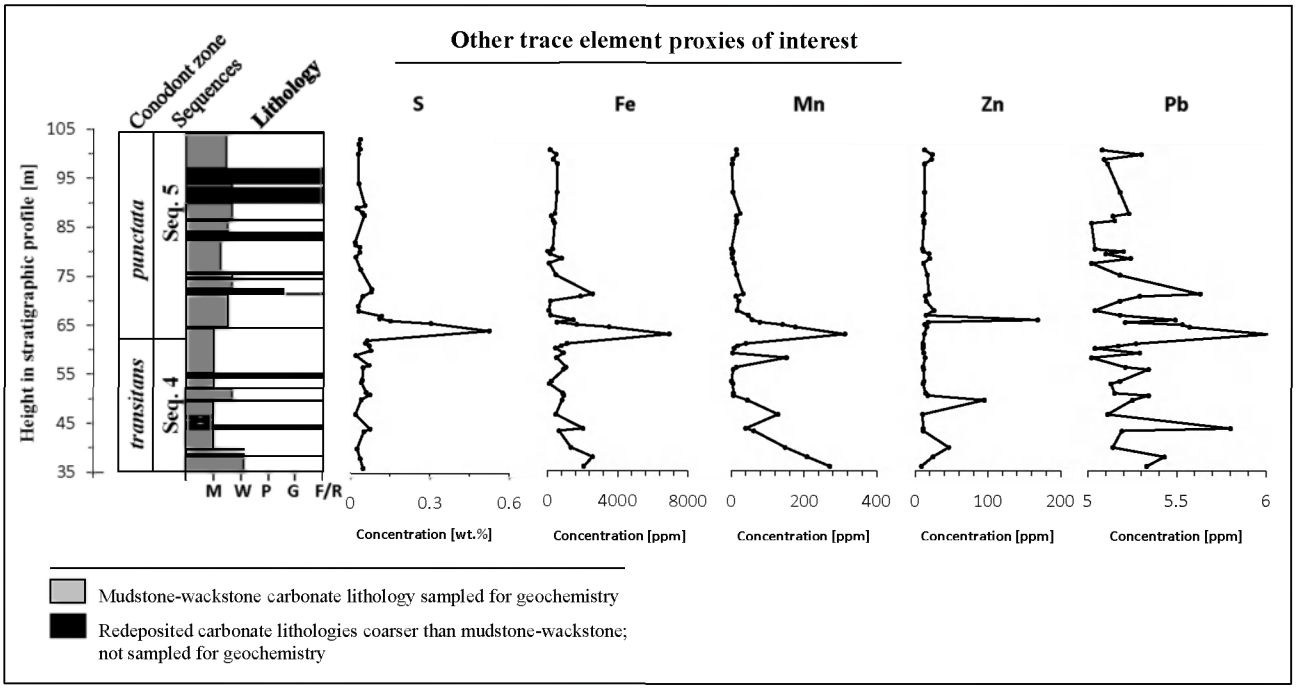


**Figure 8**. Chemostratigraphic profiles of elements used as supporting proxies for bioproductivity and redox conditions prevailing during the *punctata* Event.

2004). The calculated indices (Fig. 7) reveal oscillations which suggest changes in the oxygenation level of bottom waters from dominantly dysoxic-anoxic to intermittently oxic conditions (note that no threshold values were assigned to the U/Th redox index. The highest observed value is near 0.04 - much lower than the cutoffs determined by Jones & Manning, 1994; (Table 2)). Dominantly reducing conditions may also be inferred from the observed enrichments of the sulfide-forming (excluding Mn) supporting proxies (Zn, Pb, Fe, S - Fig. 8) and a S/Fe ratio near that of stoichiometric pyrite (Fig. 9).

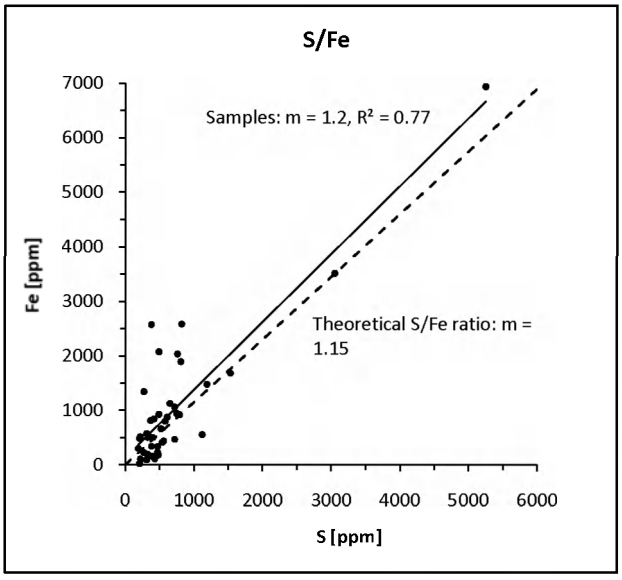


**Figure 9**. Crossplot of S versus Fe concentrations. The theoretical dashed line with a slope of 1.15 indicates that all Fe is sequestered in a pyritic phase (see discussion in Rimmer, 2004).

## 5. Discussion: TOC and Trace element enrichments: Implications for detrital input, paleobioproductivity and redox conditions

### *5.1 Changes in detrital input and MS before and during the punctata Event*

The growth and development of the Miette carbonate platform kept pace with a 2nd order sea level rise, superimposed on which are nine 3rd order transgressive-regressive cycles (T-R) (Whalen et al., 2000; Whalen & Day, 2008). The observed geochemical excursions of the *punctata* Event occur during sea level lowstand and early transgression of 3rd order transgressive pulse IIc1 (Fig. 3) (pulse IIc1 coincides with the onset of the *punctata* zone and continues into the overlying *P.hassi* zone). The IIc T-R event was identified by Johnson et al. (1985), further refined by Day (1996), Johnson et al. (1996), and Sandberg et al. (2002), and subdivided into two events – IIc1 and IIc2 – in western Canada by Whalen & Day (2008, Fig. 6). Within the framework of the four-step $\delta^{13}C$ perturbation which characterizes the *punctata* Event (see Fig. 18 in Pisarzowska et al., 2006 and Fig. 1 in Racki et al., 2008), the trace element enrichments correspond to the major positive isotopic shift (step III in Pisarzowska et al., 2006). The concentrations of detrital proxies (Al, Si, K, Ti, Cr, Zr and Co) increases prominently across the *P.transitans-P. punctata* zonal boundary and into the *punctata* zone itself. This corresponds well with magnetic susceptibility increases following a MS low during eustatic sea level highstand in the mid-*transitans* zone (cf. Whalen & Day, 2008) (Fig. 4). Ti/Al and Zr/Al ratios (Fig. 5) are interpreted to record relative variations in the sedimentation rate during this time, and record oscillations throughout

the sampled interval in tandem with MS. The Zr/Al ratio shows an inversed trend, and the use of both the Ti/Al and the Zr/Al proxies is thus inconclusive in this study. However, graphic correlation of MS trends from Section AB with three other stratigraphic profiles in the basin reveals a thicker package of sediment deposited during the *punctata* interval at Section AB, interpreted by Whalen & Day (in review) to indicate higher rates of sedimentation. The observed trace element enrichments are interpreted in part as an increase in the amount of terrigenous siliciclastic material delivered to the depositional basin during a transient intensification of continental weathering (John et al. 2008; Racki et al. 2008 and others therein). It must also be noted, however, that this detrital signal may have been amplified in part by the 3rd order scale relationships between sea level and MS developed by Whalen & Day (in review) for the Western Canada Sedimentary Basin. MS highs are observed during late highstand, lowstand and early transgression. Whalen & Day (in review) observe that because early transgressive systems commonly rework siliciclastic material originally deposited during sea level lowstands, early transgressive facies may similarly inherit higher MS signatures. In concordance with this observation, MS signatures recorded in the stratigraphic profile are seen to be high during late highstand of Sequence 4 (late *P.transitans* zone), lowstand at the Sequence 4-5 boundary (*P. transitans-P.punctata* zonal boundary) and during early transgressive pulse IIc1 of Sequence 5 (early *P.punctata* zone). While relative MS highs are thus expected in accordance with the observations of Whalen & Day (in review) and Ellwood et al. (1999) for the study area, it is also conceivable that the amount of siliciclastic material available for deposition during lowstand and reworking during early transgression was significantly increased during this period of enhanced continental weathering and paleobotanical developments taking place on land during the *punctata* Event.

Two corresponding *punctata* Event sections in Poland (Holy Cross Mountains) record two distinct pulses of increased clastic detritus delivery to the ocean basins of Central Europe (Nawrocki et al., 2008). These pulses mark the beginning and the end phases of a broad MS low which spans the *punctata* zone. Generally, eustatic sea level rises correspond to low MS values, and sea level falls are associated with increased detrital fluxes and higher MS because more continental land is exposed and subject to erosion (Ellwood et al., 1999, 2000; Whalen & Day, 2008). Nawrocki et al. (2008) thus interpreted the MS variation as a record of a general transition from relatively high to low sea-level stands near the *P. punctata-P.hassi* zonal boundary. Further, they suggested that pulses of Eovariscan tectonic uplift and erosion have enhanced the MS record they observed. The basinal facies of the Miette carbonate platform in Western Alberta record an increase in MS throughout the lower *punctata* zone. Recognizing any potential MS high at the top of this zone, as observed in Central Europe, is precluded by the covered portion of the outcrop that contains the *P.punctata-P.hassi* zonal boundary. We interpret the MS elevation in the lower *punctata* zone in part as an increase in the amount of terrigenous siliciclastic material delivered to the basin, in correspondence with sea-level lowstand at the end of T-R cycle IIb3 and early transgression of T-R cycle IIc1. MS signatures from marine sediments have been proposed for use in regional and supraregional stratigraphic correlations (Ellwood et al., 2000; Whalen & Day, 2008, Nawrocki et al., 2008 and references therein). Long-term, high magnitude and low-frequency MS events correspond to supraregional erosion associated with geographically extensive orogenic events (Ellwood et al., 1999; Nawrocki et al., 2008; Whalen & Day, 2008). Conversely, short-term, low-magnitude, high-frequency MS oscillations correspond to regional sediment shedding and may reflect climatic signatures and relative changes in sea level (Ellwood et al., 1999; Nawrocki et al., 2008; Whalen & Day, 2008). Concerning the Early to Middle Frasnian, various authors have noted and interpreted a general long-term decrease of MS magnitude as indicative of worldwide sea level transgressions and the associated decrease in detrital input (see references in Nawrocki et al., 2008). This long-term trend is also observed in the Western Canada Sedimentary Basin (Whalen & Day, 2008), superimposed on top of which are the likely regional oscillations of the *punctata* Event.

The two MS pulses in the *P.punctata* zone recorded in the Holy Cross Mountains (Poland) were interpreted to represent initial pulses of the Variscan orogeny, which uplifted the Mid-German Crystalline High (Nawrocki et al., 2008). The beginning of synorogenic sedimentation is thought to have taken place near the E-MF transition – i.e. temporally near the beginning of the *P.punctata* conodont biozone. This interpretation is supported by a pulsed increase in the seawater $^{87}Sr/^{86}Sr$ ratio throughout the *punctata* Event (John et al., 2008). While the overall Sr isotope ratio of seawater increased throughout the Middle and Late Devonian, the superimposed 'pulsed increase' within the *punctata* zone may reflect a transient increase in continental weathering associated with the initial phases of Eovariscan orogenic uplift (John et al., 2008). It is noteworthy to point out that during Middle to Late Devonian times, all the thus-far studied *punctata* Event sections, including those in the Western Canada Sedimentary Basin, were located in the equatorial paleolatitudes, where denundation of uplifted areas and rates of chemical weathering, associated with the spread of forests and advent of intense pedogenesis, would have been relatively high (cf. John et al., 2008). Our geochemical dataset displays a prominent increase in the absolute concentrations of both Rb and Sr throughout the *punctata* disturbance (Fig. 5). Sr concentrations generally increase steadily up-section, with a superimposed 'pulse,' corresponding to all other trace element enrichments (Figs 4-6). John et al. (2008) demonstrated that uniformity of $^{87}Sr/^{86}Sr$ values across all oceans of the Frasnian age is to be expected, given that the residence time of Sr in oceans is, and likely has been in past periods of geologic time, longer than oceanic mixing rates. This was evidenced by comparing values from Central European basins and those of palaeogeograhpically distant locations in South China.

Thus a rapid weathering-related flux of Sr into the oceans at one locality (i.e. the Central Europeans basins) would be recorded globally (both as an increase in the $^{87}Sr/^{86}Sr$ ratio, but also as an increase in absolute Sr concentrations). The basinal carbonates of Western Alberta could thus have recorded a mixed signal indicating regional weathering of uplifted lands but also weathering of distant orogens, such as those of Central Europe and northern Canada.

Previous work in the Alberta subsurface documented the progressive east-to-west infilling of the Western Canada Sedimentary Basin from the Late Givetian through the Fammenian (Stoakes, 1980). Frasnian siliciclastics consist of clay and silt partially derived from the Ellesmerian fold belt provenance in the Canadian Arctic Archipelago but a component of this sediment was probably eolian transported from the Laurussian continental interior (Whalen & Day, 2008). Stevenson et al. (2000) argued, based on Sm-Nd isotopic data, that the detrital provenance did not change to the westerly Antler orogeny related source areas until the Fammenian. Thus the observed increases in MS and detrital influx during the *punctata* Event cannot be explained directly by regional pulses of orogenic activity in the immediate vicinity of the depositional basin (as was done by Nawrocki et al., 2008 for the basins of Central Europe). But perhaps an intensification of weathering, in the northerly Ellesmerian Fold Belt region and the continental interior, caused by a pulse of forest expansion and a warming climate can be implicated. The advent and spread of vascular land plants of tree stature would have profoundly altered the hydrologic cycle and the course of soil development (Algeo & Scheckler, 1998). Intimate interactions of vegetation with atmospheric water would have begun altering the land surface albedo and increased precipitation while weathering substrates more thoroughly and intensely than non-vascular vegetation of the pre-Middle-Late Devonian (Algeo & Scheckler, 1998 and references therein). Weathering rates would have been all the more accelerated in wet, warm near-equatorial regions (White & Blum, 1995) and further amplified by a Frasnian climatic warming trend reconstructed using conodont apatite $\delta^{18}O$ signatures (Joachimski et al., 2009) and palynomorph assemblages (Streel et al., 2000) (however, see Fig. 1 in Racki et al. 2008 showing a reconstructed Frasnian cooling trend based on conodont apatite and Pisarzowska, 2008 for the original isotopic study).

### *5.2 Bioproductivity proxy trends*

The *punctata* Event $\delta^{13}C$ excursion was interpreted by Ma et al. (2008, p. 144) using supporting trace element geochemistry as an indicator of enhanced bioproductivity and organic matter burial during the Early-Middle Frasnian transition within the South China basin. Trace element records from the Western Canada Sedimentary Basin are consistent with this interpretation, as are changes in TOC (both for the studied stratigraphic profile (Fig. 6) but also for a correlative section in an adjacent thrust sheet - Section K; Fig. 7 in Whalen & Day, 2000). Both Cu and Ni, which have been used as direct proxies for oceanic bioproductivity (i.e. Piper & Perkins, 2004; Riquier et al., 2006; Ma et al., 2008; Perkins et al., 2008; Piper & Calvert, 2009), are appreciably enriched. Both elements behave as micronutrients (although Cu to a lesser extent than Ni) in oxic marine environments and are delivered to the sediment via complexations with OM but are also enriched via the redox cycling of Fe-Mn oxyhydroxides (Calvert & Pedersen, 1993; Tribovillard et al., 2006). Sediments with high OM fluxes are a significant sink for these metals (and also for Cd, Zn, Cr, V, Re, Mo and U). Zn also behaves as a micronutrient and is removed form surface waters by plankton growth. Its enrichment in the profile supports what is inferred from the elevated levels of Cu and Ni.

Within the context of the Algeo & Sheckler (1998) model, a transient intensification of pedogenesis and increased delivery of biolimiting nutrients (Ni, Cu, Zn, P) to the oceans may have stimulated a temporary elevation of primary productivity. High correlations between the MS, TOC, bioproductivity and detrital influx proxies (Tables 3 & 4) suggest that enhanced primary production was mainly detrital-driven. Organic matter enrichments are interpreted as a mixed signal of both increased productivity and preservation under at least intermittently reducing bottom water conditions (Murphy et al., 2000), given that strong correlations exist between TOC and the redox sensitive proxies (Tables 3 & 4). Rimmer (2004, p. 388) suggests that "different relationships between $C_{org}$ and a redox-sensitive element in adjacent units, units that most likely have experienced similar tectonic and basinal fluid influences, may suggest differing roles of anoxia during OM accumulation." Without a suitable point of comparison, however, we are at present unable to describe the relative importance of anoxia in OM accumulation. The strong correlations only confirm the intimate relationship between $C_{org}$ preservation and bottom water oxygen deficiency, but are not adequate to discern whether enhanced preservation or a greater flux of OM to the sediment was responsible for the observed organic enrichments.

Sedimentary phosphorus enrichments, as discerned in the geochemical trends (Fig. 6), are unfortunately not necessarily directly indicative of enhanced primary productivity (Tribovillard et al., 2006). Dissolved phosphate is immobilized in the sediment when the surface layer is oxic, and sequestration occurs via bioaccumulation (active phosphorus storage by microorganisms) and Fe-oxyhydroxide precipitation (which prevents P escape to the water column because of a large sorption capacity (van Cappellen & Ingall, 1994)). If the overlying water layer becomes oxygen-depleted, P is released and may diffuse back to the photic zone where it can again be utilized by the planktonic biomass. In the context of the other productivity proxies, the observed P enrichment and correlation with TOC (Tables 3 & 4) suggests increased OM fluxes to the sediment preserved during intermittently oxic bottom water conditions which favor P retention, and possible trapping in an apatite

mineral phase. While the redox proxies imply dominantly suboxic-anoxic conditions during the *punctata* Event, periodic oxia is supported by petrographic evidence – mainly bioturbation observed within some sedimentary horizons but not in others (Whalen et al., 2000).

Together with Ni, Cu and P, Ba levels are also elevated at the base of the *punctata* biozone. The enrichment is an order of magnitude higher than 'background' values in the chemostratigraphic profile, the peaks and troughs of which correspond to those of the other trace element proxies (even though these peaks and troughs are obscured by the magnitude of the Ba peak). This may be a mixed signal of Ba accumulation in a sedimentary horizon as a result of cycling across redox gradients (barium 'fronts,' as described in Dickens et al., 2003; Tribovillard et al., 2006) and increased riverine delivery of Ba to the oceans. Correlations with the detrital proxies are high (although not with MS – Tables 3 & 4), suggesting increased weathering in the sediment source areas as a partial mechanism of increased Ba delivery. The flux of Ba to oceanic surface waters is substantial (Dickens et al., 2003), and presumably would have been augmented significantly during the initial phases of terrestrial afforestation and intensification of pedogenetic processes. Once in solution, Ba precipitates within microenvironments surrounding decaying and sinking OM (Dickens et al., 2003). Increased OM and Ba levels in the euphotic zone during the *punctata* Event could have resulted in a greater export of this element to the sediment-water interface. While difficult to use as a direct bioproductivity indicator (because of it mobility under varying redox conditions; Tribovillard et al., 2006), the Ba signal, when set within the context of the other geochemical proxies, seems consistent with both an increased riverine delivery of this element and increases in primary production and export productivity (suggested by Ni, Cu and P enrichments) which may have effectively transferred inflowing Ba from the water column to the sediment.

### *5.3 Paleoredox proxy trends*

Oceanic bottom water anoxia and changes in primary productivity have been traditionally regarded as distinct processes which control the formation of organic-carbon rich sediments and sedimentary rocks (Pedersen & Calvert 1990; Canfield, 1994). Early work on ancient black shales tended to prefer one process over the other to explain the origin of such facies, whereas more recently, enhanced OM preservation under anoxic conditions and enhanced bioproductivity are viewed as two endmembers of a continuum (Murphy et al., 2000). Within a given depositional basin, the degree of influence of either end-member may shift along this continuum as time passes and oceanographic conditions change. The $C_{org}$-rich slope and basinal mudstones of the Miette carbonate platform are thus interpreted as a product of both increased primary productivity during the *punctata* Event, as indicated by enrichments of bioproductivity tracers and TOC, but also of enhanced OM preservation driven by bottom water oxygen depletion and the prevalence of reducing conditions, as evidenced by coeval enrichments of paleoredox tracers (Mo, U, V; Fig. 6). Using first order trends observed in the stratigraphic distribution of each redox index (Ni/Co, U/Th, V/Cr, V/(V+Ni)) (Fig. 7), and following the precautions outlined in Rimmer (2004), we collectively and relatively interpret these indices as further indicating dominantly suboxic-anoxic conditions throughout the *punctata* Event. Rimmer (2004) found 'fairly good agreement' when interpreting redox conditions using the threshold values for Ni/Co and V/Cr established by Jones & Manning (1994). In the present study, we found reasonable agreement likewise with the Ni/Co threshold of those same authors, and the V/(V+Ni) cutoff values of Hatch & Leventhal (1992). The V/Cr and U/Th ratios, however, despite showing prominent enrichments within the *punctata* zone consistent with the other indices, fall below the established oxic-dysoxic boundaries of the above cited studies (Fig. 7, Table 2). Our observations strengthen the arguments of Rimmer (2004) concerning strict definitions and applications of these ratio indices.

Dominantly reducing conditions in the depositional basin likely developed in the presence of sedimentary OM (high correlations of TOC and redox tracers – Tables 3 & 4). But can a distinction between water-column and sediment pore-water anoxia be made? Second-order oscillations of the redox index trends (Fig. 7) seem to indicate intermittently oxic bottom water conditions at the sediment-water interface, allowing for the accumulation of P (and in agreement with the aforementioned petrographic evidence) (via P-trapping under oxic conditions; Ingall & Jahnke, 1994, van Cappellen & Ingall, 1994, 1996; Lenton & Watson, 2000; Wallmann, 2003; Tribovillard et al., 2006). Intermittent oxygenation may have been caused by some degree of water column mixing associated with the well documented gravity flow deposits prevalent within the stratigraphic profile (Whalen et al., 2000). Following the interpretation of Riquier et al. (2006), the observed Mn enrichment (Fig. 8) can further aid the distinction between water-column and sediment pore-water anoxia. Mn and redox-sensitive, sulphide-forming element enrichments in tandem could indicate that at times the boundary between oxidizing and reducing conditions was 'pushed down' from an otherwise stratified water column to the sediment-water interface, or below it - allowing for Mn fixation (in either rhodochrosite ($MnCO_3$) or kutnahorite ($Ca(Mn,Mg,Fe)(CO_3)_2$)).

### *5.4 The punctata Event within the context of the Algeo & Sheckler (1998) model*

The Devonian marine-terrestrial teleconnections model of Algeo & Scheckler (1998) provides a theoretical framework within which the geochemical trends of the *punctata* Event may be interpreted. At the core of this model is the soil, which behaves as a geochemical interface between the lithosphere, the atmosphere and the hydrosphere. The Middle-Late Devonian is characterized by widespread oceanic bottom water anoxia, increased organic carbon burial rates and a prolonged biotic crisis that culminates in the Frasnian-Famennian mass extinction

(Racki, 2005). The rapid evolution and geographically vast expansion of soils during this time period may be the link which connects such marine events to developments in the terrestrial realm - mainly the rise, rapid diversification and expansion of vascular plants, but archaeopterid forests in particular (Algeo et al., 1995; Algeo & Scheckler, 1998). Prior to the Late Devonian, terrestrial plants were small, at most shallowly-rooted and their geographic extent was limited to moist lowland habitats by their reproductive mode (Gensel & Andrews, 1984, 1987; Thomas & Spicer, 1987). By Late Devonian time, vascular land plants (which evolved and began diversifying in the Late Silurian-Early Devonian) became arborescent (achieved tree stature) and evolved the seed habit, which allowed them to expand geographically into previously inaccessible upland habitats (Thomas & Spicer, 1987). Archaeopterids, which grew to more than 30 meters in height, achieved trunk diameters of more than 1.5 meters (Beck, 1981) and were significantly more deeply rooted than any prior plant, may have comprised monotaxic forests in floodplain habitats during the Middle to Late Frasnian. Soil penetration depths by root systems increased to 80-100 cm by the Frasnian-Fammenian, resulting in intensified pedogenesis and pedoturbation (Beck, 1967; Snigirevskaya 1984, 1995; Retallack, 1985).

The occurrence of deeply rooted palaeosols and in particular soil types associated mainly with temperate-zone forests increases in frequency during the Devonian, and has been interpreted as a reflection of forest expansion beyond floodplain habitats (Allen, 1986; Driese & Mora, 1993; Retallack, 1986, 1990, 1992). But how rapid could afforestation have been? Burnham (2008) reviewed certain aspects of the plant fossil record and contemporary plant ecology (especially records of invasive plant species spread, recolonization of volcanic areas and otherwise disturbed habitats, but also historical plant migration patterns) in an attempt to answer the following question: how rapidly do newly evolved and reasonably successful plant species increase in abundance from a few individuals to a biomass sufficiently large so as to have a high probability of representation in the fossil record? Burnham (2008) concluded that this time interval is geologically short (ca. 2000 years), and for rocks of Devonian age can be thought of as instantaneous. Algeo et al. (1995, p. 64) note that the Frasnian-Famennian (F/F) boundary Kellwasser events occurred 'within the mid-Frasnian to mid-Famennian interval of archaeopterid dominance and might represent the rapid spread of this genus." While it may be nearly impossible to tightly constrain and correlate the timing of archaeopterid forest expansion (perhaps in multiple pulses?) with marine events in the geological record (because of a lack of suitable datable materials in Devonian non-marine successions), we can speculate that the *punctata* Event, temporally near the onset of archaeopterid rise to dominance, may record the geochemical consequence of a initial pulse of afforestation.

The Algeo and Scheckler (1998) model and related studies (Wright, 1990; Berner, 1997, 1998; Scheckler, 2001; Beerling & Berner, 2005) further propose that the diversification and expansion of vascular land plants altered the nature of continental weathering via the evolution of deeply rooted palaeosols. In essence, more thorough weathering of the bedrock was initiated within the microenvironments created around the root systems of arborescent taxa. While overall sediment yields may have decreased, the landscape stabilizing properties of vegetative cover had the net result of increasing the residence time of sediment within the weathering zone, where it could be more thoroughly decomposed. This in turn would have increased the flux of readily available micronutrients delivered to the shallow oceans by riverine discharge. Such a flux of biolimiting nutrients would stimulate primary production, lead to increased burial of organic matter and thus contribute to water-column stratification via bottom water oxygen depletion.

A fundamental characteristic of this model, however, is that it very eloquently describes the dynamic but transient response of the lithosphere-atmosphere-ocean system to a rapid and aerially expansive diversification of a terrestrial biomass capable of interacting in a unprecedented way with its substrate. The large atmospheric $CO_2$ reservoir of the pre-Devonian (4-20 PAL (present atmospheric level), Berner, 1994, 2006; Berner et al., 2007) likely allowed for a rapid but pulsed diversification and expansion of forests. 'Excess' atmospheric $CO_2$ (that amount which was in excess of that supplied by fluxes into the atmosphere-ocean system by volcanic and metamorphic degassing) was consumed for increasing the terrestrial biomass and actively pumped into soils, where it stimulated a transient increase in silicate weathering (pedogenesis). Steady-state was eventually achieved with lower overall atmospheric $CO_2$ concentrations ($pCO_2$) (mid-Carboniferous $pCO_2$ around 1 PAL, Berner, 1994, 2006; Berner et al., 2007) maintained by active pumping by terrestrial vegetation and a return of silicate weathering rates to those of the pre-Devonian. It is within the context of this working model that we interpret the geochemical signatures of the *punctata* Event recorded in the basinal carbonate mudstones in the Western Canada Sedimentary Basin.

## 6. Conclusions

The *punctata* Event records one of the larger $\delta^{13}C$ excursions found to date in the rock record of the Phanerozoic. This perturbation of the global carbon cycle is accompanied by geochemical excursions, among them the suites of trace elements used as proxies for changes in detrital input, bioproductivity, and oceanic bottom water redox conditions. This event was set within the context of the rapidly changing Late Devonian world, where ecosystem readjustments eventually culminated in the Frasnian-Fammenian mass extinction, one of the five largest since the base of the Cambrian. Yet despite this apparently severe environmental perturbation, no major biotic crisis was found to be associated with the *punctata* Event.

Among other localities worldwide, a record of this geochemical event was found in the basinal facies of the

Miette carbonate platform in the Western Canada Sedimentary Basin. Using trace element proxies, MS variability and TOC determinations, we interpreted the *punctata* Event within 1) a regional sequence stratigraphic context and 2) within the framework of concurrent global changes of the Frasnian age. This dataset is intended to complement the growing body of work (summarized in Yans et al., 2007; Racki et al., 2008; Morrow et al., 2009) aimed at elucidating the causes and understanding the effects of terrestrial and marine events of the *P.punctata* biozone and, more broadly, at understanding the Earth-system changes of the Late Devonian leading up to the F/F boundary.

The stratigraphic distribution of bioproductivity, paleoredox and detrital influx proxies reveals a prominent enrichment near the onset of the *punctata* Event, beginning across the *P.transitans-P.punctata* zonal boundary and continuing above it. It coincides also with the transition between 3rd order sea level sequences 4 & 5 (Whalen & Day, 2008). The proxy suites co-vary with MS, suggesting an inherent interdependence and changes in detrital input as the main driver of the oceanographic changes which produced the observed geochemical excursions. Such covariance trends are consistent with recently developed models of MS variation during the different phases of T-R cycles within this region (Whalen & Day, in review).

The bioproductivity proxies and TOC excursions suggest that a prominent but transient increase of the planktonic biomass occurred during the *punctata* Event, allowing for the development of dominantly dysoxic to anoxic bottom water conditions (punctuated by intermittent oxia, likely associated with water column mixing during the deposition of the numerous gravity flow deposits). Given that significant statistical correlations were found among all suites of geochemical proxies, TOC and MS, this biomass growth was likely detrital-driven. While a higher influx of terrigenous siliciclastics is expected to enter the depositional basin during conditions of sea level lowstand and early transgression (during which the observed geochemical excursions took place), coeval developments on land may have amplified the oceanographic changes observed during the *punctata* Event. The climatic warming trend of the Frasnian (Joachimski et al., 2009) may have intensified the weathering of uplifted lands in the Ellesmerian fold belt (Canadian Arctic Archipelago) – a partial sediment source for the Alberta Basin. Potentially more influential, however, was the rapid rise and expansion of the first terrestrial forests (archaeopterid forests) and the evolution of complex paleosols, beginning in the mid-Frasnian. The rise of vascular, arborescent land plants would have had a profound effect on the interactions between the lithosphere, hydrosphere and the atmosphere increasing weathering rates not only in uplands but also in any forested continental area. The Algeo & Sheckler (1998) terrestrial-marine teleconnections model provides an intricate contextual framework for explaining marine events of the Late Devonian (mainly widespread bottom water anoxia and enhanced rates of organic carbon burial) by observing changes (primarily paleobotanical) taking place on the continents. The expansion of forests was accompanied by the concurrent evolution of deeply weathered and aerially expansive soils that altered solute fluxes (among them biolimiting nutrients) to the oceans via riverine discharge, allowing for increases of the planktonic biomass. While tight time constraints and correlations between the *punctata* Event and the onset of terrestrial afforestation will likely remain elusive, we can speculate that this mid-Frasnian evolutionary event contributed substantially to the observed geochemical perturbation.

## 7. Acknowledgments

This work is dedicated to Prof. B.C. Schreiber, for years of support. The authors would like to thank K.Severin and R.Newberry for constructive discussions and instrumental help in developing the specialized XRF analytical protocols used for generating the trace element data for this study. The authors would also like to thank J.Addison for insightful discussions on interpreting trace element proxies in light of near-contemporary oceanography. We also would like to acknowledge G. Racki and L. Riquier for critical review of the manuscript.

## 8. References

ALGEO, T.J. & MAYNARD, J.B., 2008. Trace-metal covariation as a guide to water-mass conditions in ancient anoxic marine environments. *Geosphere*, 4: 872-887.

ALGEO, T.J. & SCHECKLER, S.E., 1998. Terrestrial-marine teleconnections in the Devonian: links between the evolution of land plants, weathering processes, and marine anoxic events. *Philosophical Transactions of the Royal Society B-Biological Sciences*, 353: 113-128.

ALGEO, T.J., BERNER, R.A., MAYNARD, J.B. & SCHECKLER, S.E., 1995. Late Devonain oceanic anoxic events and biotic crises: "rooted" in the evolution of vascular land plants? *GSA Today*, 5: 1-66.

ALLEN, J.R.L., 1986. Pedogenic calcretes in the Old Red Sandstone facies (Late Silurian – Early Carboniferous) of the Anglo-Welsh area, southern Britain. *In* Wright, V.P. (ed.) *Paleosols: their recognition and interpretation*. Oxford: Blackwell, 58-86.

BALINSKI, A., OLEMPSKA, E. & RACKI, G., 2006. Early-Middle Frasnian transition: Biotic response to a major perturbation of the global carbon budget. *Acta Palaeontologica Polonica*, 51: 606-608.

BECK, C.B., 1967. *Eddya sullivanensis*, gen. et sp. nov., a plant of gymnospermic morphology from the Upper Devonian of New York. *Paleontographics*, B 121: 1-22.

BECK, C.B., 1981. Archaeopteris and its role in vascular plant evolution. *In* Niklas, K.J., (ed.) *Paleobotany, paleoecology, and evolution*, vol. 1., Praeger, New York.

BEERLING, D.J. & BERNER, R.A., 2005. Feedbacks and the coevolution of plants and atmospheric $CO_2$. *Proceedings of the National Academy of Sciences of the United States of America*, 102: 1302-1305.

BERNER, E.K., BERNER, R.A. & MOULTON, K.L., 2007. Plants and mineral weathering: Present and past. *In Treatise on Geochemistry*, Chapter 5.06, 169-188.

BERNER, R.A., 1994. 3GEOCARB-II - A revised model of atmospheric $CO_2$ over Phanerozoic time. *American Journal of Science*, 294: 56-91.

BERNER, R.A., 1997. Paleoclimate - The rise of plants and their effect on weathering and atmospheric $CO_2$. *Science*, 276: 544-546.

BERNER, R.A., 1998. The carbon cycle and $CO_2$ over Phanerozoic time: the role of land plants. *Philosophical Transactions of the Royal Society of London Series B-Biological Sciences*, 353: 75-81.

BERNER, R.A., 2006. GEOCARBSULF: A combined model for Phanerozoic atmospheric $O_2$ and $CO_2$. *Geochimica et Cosmochimica Acta*, 70(23): 5653-5664.

BERTRAND, P. et al., 1996. The glacial ocean productivity hypothesis: The importance of regional temporal and spatial studies. *Marine Geology*, 130: 1-9.

BURNHAM, R.J., 2008. Hide and go seek: What does presence mean in the fossil record? *Annals of the Missouri Botanical Garden*, 95: 51-71.

CALVERT, S.E. & PEDERSEN, T.F., 1993. Geochemistry of recent oxic and anoxic marine sediments - implications for the geological record. *Marine Geology*, 113(1-2): 67-88

CANFIELD, D.E., 1994. Factors influencing organic-carbon preservation in marine sediments. *Chemical Geology*, 114(3-4): 315-329

CAPUTO, M.V., 1985. Late Devonian glaciation in South America. *Palaeogeography Palaeoclimatology Palaeoecology*, 51: 291-317.

CAPUTO, M.V., 2008. Late Devonian and Early Carboniferous glacial records of South America. *Geological Society of America Special Papers*, 441: 161-173.

DA SILVA, A.C., YANS, J. & BOULVAIN, F., 2010. Early-Middle Frasnian (early late Devonian) sedimentology and magnetic susceptibility of the Ardennes area (Belgium): identification of severe and rapid sea level fluctuations. *Geologica Belgica*, this volume.

DAVIS, J.C., 2002. Statistics and Data Analysis in Geology (3rd ed.). New York: John Wiley & Sons.

DAY, J., 1996. Faunal signatures of Middle-Upper Devonian depositional sequences and sea level fluctuations in the Iowa Basin: US mid-continent. *Geological Society of America Special Papers*, 306: 277-300.

DICKENS, G.R., THOMAS, E. & BRALOWER, T.J., 2003. Excess barite accumulation during the Paleocene-Eocene Thermal Maximum: Massive input of dissolved barium from seafloor gas hydrate reservoirs. *Geological Society of America Special Papers*, 369: 11-23.

DRIESE, S.G. & MORA, C.I., 1993. Physico-chemical environment of pedogenic carbonate formation in Devonian vertic palaeosols, central Appalachians, USA. *Sedimentology*, 40: 199-216.

ECHARFAOUI, H., HAFID, M. & SALEM, A.A., 2002. Seismic structure of the Doukkala basin, Palaeozoic basement, western Morocco: a hint for an Eovariscan fold-and-thrust belt. *Comptes Rendus Geoscience*, 334: 13-20.

ELLWOOD, B.B., CRICK, R.E. & EL HASSANI, A., 1999. The magneto-susceptibility event and cyclostratigraphy (MSEC) method used in geological correlation of Devonian rocks from Anti-Atlas Morroco. *American Association of Petroleum Geologists Bulletin*, 83: 1119-1134.

ELLWOOD, B.B., CRICK, R.E., EL HASSANI, A., BENOIST, S.L., & YOUNG, R.H., 2000. Magnetosusceptibility event and cyclostratigraphy method applied to marine rocks: Detrital input versus carbonate productivity. *Geology*, 28: 1135-1138.

ELRICK, M., BERKYOVA, S., KLAPPER, G., SHARP, Z., JOACHIMSKI, M., & FRYDA, J., 2009. Stratigraphic and oxygen isotope evidence for My-scale glaciation driving eustasy in the Early-Middle Devonian greenhouse world. *Palaeogeography Palaeoclimatology Palaeoecology*, 276: 170-181.

GENSEL, P.G. & ANDREWS, H.N., 1984. *Plant life in the Devonian*. New York: Praeger.

GENSEL, P.G. & ANDREWS, H.N., 1987. The evolution of early land plants. *American Scientist*, 75: 478-489.

GELDSETZER, H.H.J., 1989. Ancient Wall reef complex, Frasnian age, Alberta. *In* Geldsetzer, H.H.J., James, N.P. & Tebbutt, G.E. (eds), *Reefs, Canada and Adjacent Areas*, *Canadian Society of Petroleum Geologists, Memoir*, 13: 431-439.

HATCH, J.R. & LEVENTHAL, J.S., 1992. Relationship between inferred redox potential of the depositional environment and geochemistry of the Upper Pennsylvanian (Missourian) Stark Shale Member of the Dennis Limestone, Wabaunsee Country, Kansas, U.S.A. *Chemical Geology*, 99: 65-82.

HOLMDEN, C., BRAUN, W.K., PATTERSON, W.P., EGLINGTON, B.M., PROKOPIUK, T.C., & WHITTAKER, S., 2006. Carbon isotope chemostratigraphy of Frasnian sequences in Western Canada. *Saskatchewan Geological Survery, Summary of Investigration*, 1: 1-6.

HOUSE, M.R., 2002. Strength, timing, setting and cause of mid-Palaeozoic extinctions. *Palaeogeography Palaeoclimatology Palaeoecology*, 181: 5-25.

INGALL, E. & JAHNKE, R., 1994. Evidence for enhanced phosphorus regeneration from marine sediments overlain by oxygen depleted waters. *Geochimica et Cosmochimica Acta*, 58: 2571-2575.

JOACHIMSKI, M.M., BREISIG, S., BUGGISCH, W., TALENT, J.A., MAWSON, R., GEREKE, M., MORROW, J.R., DAY, J., & WEDDIGE, K., 2009. Devonian climate and reef evolution: Insights from oxygen isotopes in apatite. *Earth and Planetary Science Letters*, 284: 599-609.

JOHN, E.H., CLIFF, R. & WIGNALL, P.B., 2008. A positive trend in seawater Sr-87/Sr-86 values over the Early-Middle Frasnian boundary (Late Devonian) recorded in well-preserved conodont elements from the Holy Cross Mountains, Poland. *Palaeogeography Palaeoclimatology Palaeoecology*, 269: 166-175.

JOHNSON, J.G., KLAPPER, G. & ELRICK, M., 1996. Devonian transgressive-regressive cycles and biostratigraphy, northern Antelope Range, Nevada: Establishment of reference horizons for global cycles. *Palaios*, 11: 3-14.

JOHNSON, J.G., KLAPPER, G. & SANDBERG, C.A., 1985. Devonian eustatic fluctuations in Euramerica. *Geological Society of America Bulletin*, 96: 567-587.

JONES, B. & MANNING, D.A.C., 1994. Comparison of geochemical indices used for the interpretation of paleoredox conditions in ancient mudstone. *Chemical Geology*, 111: 111-129.

KAUFMANN, B., 2006. Calibrating the Devonian time scale: A synthesis of U-PbID-TIMS ages and conodont stratigraphy. *Earth-Science Reviews*, 76: 175-190.

KASIG, W. & WILDER, H., 1983. The sedimentary development of the Western Rheinisches Schiefergebirge and the Ardennes (Germany/Belgium). *In* Martin, H. & Eder, F.W. (eds) *Intercontinental Fold Belts*. Springer, Berlin. 185-209.

KLAPPER, G., 1989. The Montagne Noire Frasnian (Upper Devonian) conodont succession. *Memoirs of the Canadian Society of Petroleum Geologists*, 14: 449-459

KLOVAN, J.E., 1964. Facies analysis of the Redwater reef complex, Alberta. Canada *Bulletin of Canadian Petroleum Geology*, 12: 1-100.

LENTON, T.M. & WATSON, A.J., 2000. Redfield revisited 1. Regulation of nitrate, phosphate, and oxygen in the ocean. *Global Biogeochemical Cycles*, 14: 225-248.

MA, X.P., WANG, C.Y., RACKI, G. & Racka, M., 2008. Facies and geochemistry across the Early-Middle Frasnian transition (Late Devonian) on South China carbonate shelf: Comparison with the Polish reference succession. *Palaeogeography Palaeoclimatology Palaeoecology*, 269: 130-151.

MARYNOWSKI, L., FILIPIAK, P. & PISARZOWSKA, A., 2008. Organic geochemistry and palynofacies of the Early-Middle Frasnian transition (Late Devonian) of the Holy Cross Mountains, Southern Poland. *Palaeogeography Palaeoclimatology Palaeoecology*, 269: 152-165.

MATTE, P., 2001. The Variscan collage and orogeny (480-290 Ma) and the tectonic definition of the Armorica microplate: a review. *Terra Nova*, 13: 122-128.

McLAREN, D.J., 1982. Frasnian-Famennian extinction. *Geological Society of America Special Papers*, 190: 477-484.

McLAREN, D.J. & GOODFELLOW, W.D., 1990. Geological and biological consequences of giant impacts. *Annual Review of Earth and Planetary Sciences*, 18: 123-171.

MORROW, J.R., SANDBERG, C.A., MALKOWSKI, K. & JOACHIMSKI, M.M., 2009. Carbon isotope chemostratigraphy and precise dating of middle Frasnian (lower Upper Devonian) Alamo Breccia, Nevada, USA. *Palaeogeography, Palaeoclimatology, Palaeoecology*, 282: 105-118.

MOULTON, K.L. & BERNER, R.A., 1998. Quantification of the effect of plants on weathering: Studies in Iceland. *Geology*, 26: 895-898.

MOUNTJOY, E.W., 1989. Miette Reef Complex (Frasnian), Jasper National Park, Alberta. *Memoirs of the Canadian Society of Petroleum Geologists*, 13: 497-505.

MURPHY, A.E., SAGEMAN, B.B., HOLLANDER, D.J., LYONS, D.J., & BRETT, C.E., 2000. Black shale deposition and faunal overturn in the Devonian Appalachian basin: Clastic starvation, seasonal water-column mixing, and efficient biolimiting nutrient recycling. *Paleoceanography*, 15: 280-291.

NAWROCKI, J., POLECHONSKA, O. & WERNER, T., 2008. Magnetic susceptibility and selected geochemical-mineralogical data as proxies for Early to Middle Frasnian (Late Devonian) carbonate depositional settings in the Holy Cross Mountains, southern Poland. *Palaeogeography Palaeoclimatology Palaeoecology*, 269: 176-188.

OLIVER, T.A. & COWPER, N.W., 1963. Depositional environments of the Ireton Formation, central Alberta. *Bulletin of Canadian Petroleum Geology*, 11: 183-202.

PEDERSEN, T.F. & CALVERT, S.E., 1990. Anoxia vs productivity - what controls the formation of organic-carbon-rich sediments and sedimentary rocks? *AAPG Bulletin-American Association of Petroleum Geologists*, 74: 454-466.

PERKINS, R.B., PIPER, D.Z. & MASON, C.E., 2008. Trace-element budgets in the Ohio/Sunbury shales of Kentucky: Constraints on ocean circulation and primary productivity in the Devonian-Mississippian Appalachian Basin. *Palaeogeography Palaeoclimatology Palaeoecology*, 265: 14-29.

PIPER, D.Z. & CALVERT, S.E., 2009. A marine biogeochemical perspective on black shale deposition *Earth-Science Reviews*, 95: 63-96.

PIPER, D.Z. & PERKINS, R.B., 2004. A modem vs. Permian black shale - the hydrography, primary productivity, and water-column chemistry of deposition. *Chemical Geology*, 206: 177-197.

PISARZOWSKA, A., 2008. Geochemia stabilnych izotopów węgla i tlenu na pograniczu dolnego i środkowego franu (dewon górny) na obszarze południowego szelfu Laurussi. PhD. Thesis, Silesian University, Sosnowiec, Poland.

PISARZOWSKA, A., SOBSTEL, M. & RACKI., G., 2006. Conodont-based event stratigraphy of the Early-Middle Frasnian transition on the South Polish carbonate shelf. *Acta Palaeontologica Polonica*, 51(4): 609-646.

RACKI, G., 2004. Geochemical and ecological aspects of lower Frasnian pyrite-ammonoid level at Kostomłoty (Holy Cross Mountains, Poland). *Geological Quarterly*, 48(3): 267-282.

RACKI, G., 2005. Toward understanding Late Devonian global events: few answers, many questions. *In* Over, D.J., Morrow, J.R. & Wignall, P.B. (eds) *Understanding Late Devonian and Permian-Triassic biotic and climatic events: Towards an integrated approach*. Elsevier, B.V., Chapter 2: 5-36

RACKI, G., JOACHIMSKI, M.M. & MORROW, J.R., 2008. A major perturbation of the global carbon budget in the Early-Middle Frasnian transition (Late Devonian) – Preface. *Palaeogeography Palaeoclimatology Palaeoecology*, 269: 127-129.

RETALLACK, G.J., 1985. Fossil soils as grounds for interpreting the advent of large plants and animals on land. *Philosophical Transactions of the Royal Society of London B*, 309: 105-142.

RETALLACK, G.J., 1986. The fossil record of soils. *In* Wright, V.P. (ed.) *Paleosols: their recognition and interpretation*, Princeton University Press, 1-57.

RETALLACK, G.J., 1990. Soils of the past. London: Unwin-Hyman

RETALLACK, G.J., 1992. Paleozoic paleosols. *In* Martini, I.P. & Chesworth, W. (eds) *Weathering, soils and paleosols*, Amsterdam: Elsevier B.V., 543-564.

RIMMER, S.M., 2004. Geochemical paleoredox indicators in Devonian-Mississippian black shales, central Appalachian basin (USA). *Chemical Geology*, 206: 373-391.

RIMMER, S.M., THOMPSON, J.A., GOODNIGHT, S.A. & ROBL, T.L., 2004. Multiple controls on the preservation of organic matter in Devonian-Mississippian marine black shales: geochemical and petrographic evidence. *Palaeogeography Palaeoclimatology Palaeoecology*, 215: 125-154.

RIQUIER, L., TRIBOVILLARD, N., AVERBUCH, O., DEVLEESCHOUWER, X. & RIBOULLEAU, A., 2006. The Late Frasnian Kellwasser horizons of the Harz Mountains (Germany): Two oxygen-deficient periods resulting from different mechanisms. *Chemical Geology*, 233: 137-155.

SANDBERG, C.A., MORROW, J.R. & ZIEGLER, W., 2002. Late Devonian sea-level changes, catastrophic events, and mass extinctions. *Geological Society of America Special Papers*, 356: 473-487

SAVOY, L.E., STEVENSON, R.K. & MOUNTJOY, E.W., 2000. Provenance of Upper Devonian-Lower Carboniferous miogeoclinal strata, southeastern Canadian Cordillera: Link between tectonics and sedimentation. *Journal of Sedimentary Research*, 70: 181-193.

SCHECKLER, S.E., 2001. Major Events in the History of Life: Palaeozoic Events: Afforestation - the First Forests. *In* Briggs, D.E.G. & Crowther, P.R. (eds) *Palaeobiology II*, Blackwell Science, Oxford.

SNIGIREVSKAYA, N.S., 1984. Root system of archaeopterids from the Upper Devonian od Donetz Basin (In Russian). *Annual Report All-Union Paleontology Society* (Academy of Sciences, USSR), 27: 28-41

SNIGIREVSKAYA, N.S., 1995. Archaeopterids and their role in the land plant cover evolution (in Russian). *Botanicheskii Zhournal*, 80: 70-75.

STEARN, C.W., 1987. Effect of the Frasnian-Famennian extinction event on the stromatoporoids, *Geology*, 15: 677-679.

STEVENSON, R.K., WHITTAKER, S. & MOUNTJOY, E.W., 2000. Geochemical and Nd isotopic evidence for sedimentary-source changes in the Devonian miogeocline of the southern Canadian Cordillera. *Geological Society of America Bulletin*, 112: 531-539.

STOAKES, F.A., 1980. Nature and control of shale basin fill and its effect on reef growth and termination: Upper Devonian Duvernay and Ireton Formations of Alberta, Canada. *Bulletin of Canadian Petroleum Geology*, 28: 345-410.

STREEL, M., CAPUTO, M.V., LOBOZIAK, S. & MELO, J.H.G., 2000. Late Frasnian-Famennian climates based on palynomorph analyses and the question of the Late Devonian glaciations. *Earth-Science Reviews*, 52: 121-173.

SWITZER, S.B., HOLLAND, W.G., CHRISTIE, G.S., GRAF, G.C., HEDINGER, A.S., Mcauley, R.J., WIERZBICKI, R.A., & PACKARD, J.J., 1994. Devonian Woodben-Winterburn strata of the western Canada sedimentary basin. *In* Mossop, G. & Shetsen, I. (eds) *Geological Atlas of the Western Canada Sedimentary Basin: Canadian Society of Petroleum Geologists and Alberta Research Council*, 165-202

TAIT, J.A., BACHTADSE, V., FRANKE, W. & SOFFEL, H.C., 1997. Geodynamic evolution of the European Variscan fold belt: palaeomagnetic and geological constraints. *Geologische Rundschau*, 86: 585-598.

THOMAS, B.A. & Spicer, R.A., 1987. The evolution and paleobiology of land plants. London: Croom Helm.

TRIBOVILLARD, N., ALGEO, T.J., LYONS, T. & RIBOULLEAU, A., 2006. Trace metals as paleoredox and paleoproductivity proxies: An update. *Chemical Geology*, 232: 12-32.

TRIBOVILLARD, N., AVERBUCH, O., DEVLEESCHOUWER,X.,RACKI,G.&RIBOULLEAU, A., 2004. Deep-water anoxia over the Frasnian-Famennian boundary (La Serre, France): a tectonically induced oceanic anoxic event? *Terra Nova*, 16: 288-295.

TUCKER, M.E., 2001. *Sedimentary Petrology*. Blackwell Science, Oxford.

VAN BUCHEM, F.S.P., EBERLI, G.P., WHALEN, M.T., MOUNTJOY, E.W., & HOMEWOOD, P.W., 1996. The basinal geochemical signature and platform margin geometries in the Upper Devonian mixed carbonate-siliciclastic system of western Canada. *Bulletin de la Société Géologique de France*, 167: 685-699.

VAN CAPPELLEN, P. & INGALL, E.D., 1994. Benthic phosphorus regeneration, net primary production, and ocean anoxia - a model of the coupled marine biogeochemical cycles of carbon and phosphorus. *Paleoceanography*, 9: 677-692.

VAN CAPPELLEN, P. & INGALL, E.D., 1996. Redox stabilization of the atmosphere and oceans by phosphorus-limited marine productivity. *Science*, 271: 493-496.

VAN DER WEIJDEN, C.H., 2002. Pitfalls of normalization of marine geochemical data using a common divisor. *Marine Geology*, 184: 167-187.

VAN LOON, A.J., 1999. The meaning of 'abruptness' in the geological past, *Earth-Science Reviews*, 45, 209-214.

VEIZER, J., 1983. Trace elements and isotopes in sedimentary carbonates. *Reviews in Mineralogy: Carbonates: Mineralogy and Chemistry*, 11: 265-299.

VEIZER, J., 1989. Strontium isotopes in seawater through time. *Annual Review of Earth and Planetary Sciences*, 17: 141-167.

WALLMANN, K., 2003. Feedbacks between oceanic redox states and marine productivity: A model perspective focused on benthic phosphorus cycling. *Global Biogeochemical Cycles*, 17: 18.

WHALEN, M.T. & DAY, J.E., 2008. Magnetic susceptibility, biostratigraphy, and sequence stratigraphy: insights into Devonian carbonate platform development and basin infilling, western Alberta, Canada. *Society for Sedimentary Geology*, 89: 291-314.

WHALEN, M.T. & DAY, J.E., *In review*. Cross-basin variations in magnetic susceptibility influenced by changing sea level, paleogeography and climate, Upper Devonian Western Canada Sedimentary Basin.

WHALEN, M.T., EBERLI, G.P., VAN BUCHEM, F.S.P., MOUNTJOY, E.W. & HOMEWOOD, P.W., 2000. Bypass margins, basin-restricted wedges, and platform-to-basin correlation, Upper Devonian, Canadian Rocky Mountains: Implications for sequence stratigraphy of carbonate platform systems. *Journal of Sedimentary Research*, 70: 913-936.

WHITE, A.F. & BLUM, A.E., 1995. Effects of climate on chemical-weathering in watersheds. *Geochimica et Cosmochimica Acta*, 59: 1729-1747.

WILDER, H., 1994. Death of Devonian reefs – implications and further investigations. *Courier Forschungsinstitut Senckenberg*, 172: 241-247.

WRIGHT, V.P., 1990. Major Events in the History of Life: Terrestrialization: Soils. *In* Briggs, D.E.G. & Crowther, P.R. (eds), *Palaeobiology*. Blackwell Science, Oxford. 57-59

YANS, J., CORFIELD, R.M., RACKI, G. & PREAT, A., 2007. Evidence for perturbation of the carbon cycle in the Middle Frasnian *punctata* Zone (Late Devonian). *Geological Magazine*, 144 : 263-270.

Manuscript received 20.12.2009, accepted in revised form 04.05.2010, available on line 25.06.2010

| Sample | Na (%) | Mg (%) | Al (%) | Si (%) | P (%) | S (%) | K (%) | Ti (ppm) | V (ppm) |
|---|---|---|---|---|---|---|---|---|---|
| **pE 103.0** | 0.036 | 0.151 | 0.025 | 0.673 | 0.018 | 0.039 | 0.051 | 1.3 | 1.6 |
| **pE 102.0** | 0.032 | 0.625 | 0.097 | 2.918 | 0.028 | 0.033 | 0.104 | 18.6 | 4.2 |
| **pE 101.0** | 0.039 | 0.183 | 0.092 | 1.730 | 0.026 | 0.038 | 0.123 | 19.4 | 6.4 |
| **pE 100.0** | 0.036 | 0.198 | 0.087 | 3.354 | 0.020 | 0.031 | 0.110 | 22.3 | 3.0 |
| **pE 94.0** | 0.052 | 0.227 | 0.102 | 0.887 | 0.022 | 0.033 | 0.120 | 21.6 | 3.1 |
| **pE 89.5** | 0.044 | 0.229 | 0.081 | 0.983 | 0.020 | 0.056 | 0.078 | 29.9 | 2.9 |
| **pE 89.0** | 0.037 | 0.424 | 0.019 | 4.786 | 0.017 | 0.027 | 0.028 | 2.1 | 1.8 |
| **pE 88.0** | 0.037 | 0.238 | 0.044 | 0.748 | 0.018 | 0.047 | 0.060 | 14.8 | 2.1 |
| **pE 87.5** | 0.036 | 0.313 | 0.094 | 1.009 | 0.024 | 0.054 | 0.112 | 30.2 | 2.5 |
| **pE 82.0** | 0.035 | 0.267 | 0.024 | 4.956 | 0.017 | 0.019 | 0.040 | 0.9 | 2.6 |
| **pE 81.5** | 0.034 | 0.112 | 0.016 | 0.610 | 0.017 | 0.021 | 0.027 | 0.2 | 2.1 |
| **pE 81.0** | 0.035 | 0.184 | 0.042 | 0.876 | 0.019 | 0.037 | 0.067 | 5.2 | 3.2 |
| **pE 80.0** | 0.036 | 0.225 | 0.216 | 2.290 | 0.022 | 0.037 | 0.290 | 45.6 | 4.8 |
| **pE 79.0** | 0.033 | 0.125 | 0.023 | 0.826 | 0.017 | 0.022 | 0.041 | 3.5 | 2.4 |
| **pE 76.5** | 0.034 | 1.550 | 0.030 | 0.972 | 0.021 | 0.040 | 0.060 | 5.1 | 2.4 |
| **pE 72.5** | 0.052 | 0.279 | 0.734 | 3.463 | 0.038 | 0.082 | 0.795 | 183.2 | 15.3 |
| **pE 72.0** | 0.051 | 0.280 | 0.493 | 2.957 | 0.025 | 0.081 | 0.621 | 104.6 | 7.5 |
| **pE 71.0** | 0.057 | 0.203 | 0.041 | 1.126 | 0.024 | 0.048 | 0.072 | 11.5 | 3.3 |
| **pE 69.0** | 0.038 | 0.124 | 0.019 | 0.564 | 0.023 | 0.031 | 0.037 | 1.0 | 2.8 |
| **pE 68.0** | 0.036 | 1.218 | 0.056 | 1.863 | 0.019 | 0.033 | 0.090 | 5.1 | 2.8 |
| **pE 67.0** | 0.044 | 0.649 | 0.191 | 5.355 | 0.033 | 0.119 | 0.196 | 38.6 | 14.3 |
| **pE 66.5** | 0.035 | 0.155 | 0.081 | 1.425 | 0.047 | 0.112 | 0.121 | 25.6 | 6.5 |
| **pE 66.0** | 0.041 | 0.252 | 0.254 | 2.241 | 0.028 | 0.153 | 0.319 | 81.2 | 4.6 |
| **pE 65.5** | 0.047 | 0.463 | 0.390 | 4.929 | 0.031 | 0.305 | 0.465 | 115.6 | 6.4 |
| **pE 64.0** | 0.069 | 1.414 | 1.303 | 10.359 | 0.037 | 0.525 | 1.291 | 493.3 | 19.2 |
| **pE 62.0** | 0.041 | 0.276 | 0.327 | 4.616 | 0.024 | 0.065 | 0.379 | 72.3 | 14.3 |
| **pE 61.5** | 0.044 | 0.454 | 0.200 | 2.109 | 0.024 | 0.058 | 0.291 | 61.0 | 5.4 |
| **pE 61.0** | 0.042 | 0.316 | 0.142 | 1.289 | 0.024 | 0.072 | 0.197 | 38.1 | 5.5 |
| **pE 60.0** | 0.040 | 0.334 | 0.198 | 3.964 | 0.022 | 0.079 | 0.223 | 52.3 | 8.4 |
| **pE 59.0** | 0.042 | 12.595 | 0.023 | 0.649 | 0.016 | 0.022 | 0.027 | 5.3 | 5.1 |
| **pE 57.0** | 0.042 | 0.547 | 0.424 | 3.209 | 0.024 | 0.072 | 0.524 | 105.4 | 6.0 |
| **pE 56.5** | 0.037 | 0.256 | 0.088 | 1.592 | 0.020 | 0.049 | 0.137 | 18.5 | 2.7 |
| **pE 54.0** | 0.037 | 0.333 | 0.064 | 1.073 | 0.022 | 0.047 | 0.097 | 15.4 | 3.9 |
| **pE 53.5** | 0.037 | 0.481 | 0.040 | 0.829 | 0.021 | 0.043 | 0.076 | 8.8 | 2.6 |
| **pE 51.5** | 0.035 | 0.280 | 0.196 | 2.215 | 0.025 | 0.061 | 0.257 | 46.8 | 7.0 |
| **pE 51.0** | 0.036 | 0.288 | 0.243 | 1.846 | 0.022 | 0.075 | 0.306 | 70.5 | 4.6 |
| **pE 50.0** | 0.041 | 0.758 | 0.063 | 8.381 | 0.026 | 0.042 | 0.052 | 12.9 | 3.6 |
| **pE 47.0** | 0.068 | 6.788 | 0.016 | 0.484 | 0.017 | 0.021 | 0.028 | 1.4* | 1.9 |
| **pE 44.0** | 0.034 | 0.142 | 0.411 | 2.530 | 0.016 | 0.076 | 0.516 | 76.5 | 3.6 |
| **pE 43.5** | 0.038 | 1.166 | 0.084 | 0.951 | 0.021 | 0.052 | 0.116 | 22.3 | 2.7 |
| **pE 40.0** | 0.048 | 12.889 | 0.033 | 0.533 | 0.014 | 0.027 | 0.057 | 11.7 | 1.8 |
| **pE 38.0** | 0.050 | 11.337 | 0.378 | 1.791 | 0.020 | 0.038 | 0.466 | 150.2 | 5.2 |
| **pE 36.0** | 0.035 | 12.195 | 0.356 | 2.029 | 0.023 | 0.049 | 0.512 | 163.6 | 6.0 |

**Appendix A**. Major and trace element abundances for stratigraphic SectionAB generated determined by XRF analysis (*punctata* Event, Early-Middle Frasnian Transition, Late Devonian, Western Canada Sedimentary Basin, Western Alberta, Canada).

| Sample | Cr (ppm) | Mn (ppm) | Fe (ppm) | Co (ppm) | Ni (ppm) | Cu (ppm) | Zn (ppm) | Sr (ppm) | Zr (ppm) |
|---|---|---|---|---|---|---|---|---|---|
| **pE 103.0** | 3.2 | 13.3 | 160.5 | 0.5 | 1.6 | 6.5 | 12.5 | 214.5 | 17.9 |
| **pE 102.0** | 13.3 | 14.4 | 505.9 | 0.6 | 3.6 | 7.7 | 22.9 | 147.4 | 11.8 |
| **pE 101.0** | 5.2 | 3.4 | 338.8 | 0.9 | 5.0 | 7.0 | 22.0 | 264.0 | 22.1 |
| **pE 100.0** | 7.3 | 2.2 | 574.4 | 0.5 | 3.9 | 7.0 | 12.6 | 231.4 | 20.7 |
| **pE 94.0** | 4.1 | 3.9 | 553.8 | 0.3 | 3.1 | 7.6 | 12.6 | 234.4 | 19.7 |
| **pE 89.5** | 3.5 | 23.9 | 439.4 | 0.3 | 3.0 | 5.9 | 12.1 | 202.8 | 18.8 |
| **pE 89.0** | 6.9 | 13.4 | 223.6 | 0.6 | 2.0 | 5.8 | 10.3 | 164.5 | 12.4 |
| **pE 88.0** | 3.4 | 14.1 | 335.9 | 0.6 | 2.3 | 5.9 | 11.2 | 181.1 | 15.5 |
| **pE 87.5** | 3.8 | 13.7 | 415.6 | 0.5 | 3.0 | 6.6 | 11.8 | 168.1 | 15.4 |
| **pE 82.0** | 12.5 | 0.4 | 300.5 | 0.4 | 1.4 | 5.3 | 9.8 | 143.1 | 11.0 |
| **pE 81.5** | 1.7 | 4.1 | 26.1 | 0.3 | 2.3 | 5.7 | 10.9 | 128.0 | 9.3 |
| **pE 81.0** | 2.3 | -0.5 | 165.8 | 0.3 | 3.8 | 5.4 | 18.7 | 173.6 | 14.3 |
| **pE 80.0** | 4.1 | 2.9 | 813.9 | 0.2 | 5.1 | 7.2 | 19.4 | 233.6 | 21.4 |
| **pE 79.0** | 1.9 | 7.8 | 105.1 | 0.9 | 2.3 | 6.2 | 11.1 | 156.8 | 13.0 |
| **pE 76.5** | 3.1 | 15.0 | 502.0 | 0.3 | 3.5 | 5.6 | 16.3 | 125.1 | 9.5 |
| **pE 72.5** | 13.3 | 32.3 | 2584.9 | 0.9 | 17.9 | 15.5 | 18.7 | 306.2 | 32.3 |
| **pE 72.0** | 6.4 | 12.3 | 1894.1 | 0.5 | 9.0 | 12.5 | 13.6 | 322.9 | 30.2 |
| **pE 71.0** | 1.6 | 20.3 | 181.2 | 0.5 | 4.6 | 7.0 | 14.8 | 250.3 | 20.4 |
| **pE 69.0** | 2.3 | 15.6 | 91.9 | 0.2 | 2.9 | 5.5 | 25.4 | 213.5 | 17.2 |
| **pE 68.0** | 2.3 | 45.7 | 190.6 | 0.8 | 2.8 | 4.9 | 14.5 | 133.1 | 10.7 |
| **pE 67.0** | 11.7 | 57.0 | 1479.4 | 0.6 | 10.5 | 10.4 | 168.3 | 170.1 | 14.1 |
| **pE 66.5** | 4.3 | 78.5 | 555.2 | 0.4 | 7.8 | 7.1 | 17.2 | 222.9 | 18.8 |
| **pE 66.0** | 4.6 | 141.2 | 1683.7 | 0.5 | 5.7 | 8.0 | 12.7 | 303.3 | 29.2 |
| **pE 65.5** | 7.4 | 175.9 | 3516.0 | 1.3 | 13.6 | 10.0 | 15.6 | 392.9 | 36.7 |
| **pE 64.0** | 17.4 | 312.7 | 6942.3 | 1.7 | 12.9 | 15.2 | 12.4 | 269.0 | 42.1 |
| **pE 62.0** | 8.3 | 39.9 | 1126.1 | 0.6 | 7.8 | 9.6 | 10.4 | 322.9 | 29.4 |
| **pE 61.5** | 4.3 | 16.8 | 801.3 | 0.5 | 6.1 | 8.3 | 10.9 | 389.5 | 33.7 |
| **pE 61.0** | 3.7 | 7.7 | 468.7 | 0.4 | 4.5 | 6.9 | 10.4 | 375.4 | 32.0 |
| **pE 60.0** | 10.3 | 3.7 | 919.9 | 0.8 | 5.5 | 7.2 | 11.5 | 505.9 | 43.8 |
| **pE 59.0** | 4.0 | 151.7 | 519.4 | 1.4 | 0.0 | 2.2 | 13.4 | 27.4 | 0.9 |
| **pE 57.0** | 7.1 | 13.6 | 1062.1 | 0.7 | 6.9 | 9.5 | 10.6 | 369.5 | 34.2 |
| **pE 56.5** | 6.4 | 5.0 | 925.6 | 0.7 | 3.5 | 7.2 | 11.4 | 422.0 | 35.4 |
| **pE 54.0** | 4.5 | 0.1 | 234.1 | 0.1 | 3.5 | 7.3 | 11.7 | 233.4 | 19.5 |
| **pE 53.5** | 2.0 | 4.2 | 113.3 | 0.5 | 3.3 | 6.8 | 10.5 | 219.9 | 17.6 |
| **pE 51.5** | 5.8 | 5.9 | 877.6 | 0.3 | 5.0 | 9.3 | 14.1 | 240.3 | 20.8 |
| **pE 51.0** | 5.5 | 5.9 | 945.9 | 0.6 | 5.3 | 9.6 | 17.1 | 286.8 | 26.4 |
| **pE 50.0** | 17.9 | 44.0 | 844.7 | 0.8 | 2.9 | 7.7 | 95.0 | 177.2 | 13.7 |
| **pE 47.0** | 2.4 | 128.4 | 488.1 | 1.0 | 1.2 | 4.0 | 10.0 | 61.3 | 3.7 |
| **pE 44.0** | 5.3 | 39.3 | 2037.4 | 1.1 | 3.1 | 7.4 | 11.0 | 115.6 | 11.3 |
| **pE 43.5** | 3.3 | 61.3 | 663.0 | 0.3 | 1.9 | 5.7 | 11.0 | 112.8 | 9.3 |
| **pE 40.0** | 3.0 | 148.0 | 1342.2 | 1.3 | 0.0 | 3.1 | 45.9 | 41.1 | 2.2 |
| **pE 38.0** | 5.4 | 208.6 | 2575.0 | 1.5 | 1.9 | 3.3 | 24.3 | 52.9 | 7.2 |
| **pE 36.0** | 5.9 | 270.8 | 2076.6 | 1.5 | 1.4 | 3.1 | 8.4 | 36.7 | 6.3 |

| Sample | Mo (ppm) | Ba (ppm) | Ca (%) | Rb (ppm) | Pb (ppm) | Th (ppm) | U (ppm) |
|---|---|---|---|---|---|---|---|
| **pE 103.0** | 1.5 | 3.0 | 76.9 | 5.7 | 5.1 | 78.2 | 0.6 |
| **pE 102.0** | 1.5 | 8.7 | 69.5 | 6.1 | 5.3 | 77.2 | 0.8 |
| **pE 101.0** | 1.7 | 6.5 | 73.5 | 6.2 | 5.1 | 78.7 | 0.8 |
| **pE 100.0** | 1.7 | 2.5 | 69.1 | 6.2 | 5.1 | 77.2 | 0.6 |
| **pE 94.0** | 1.6 | 5.5 | 76.1 | 6.7 | 5.2 | 82.0 | 0.4 |
| **pE 89.5** | 1.5 | 6.2 | 75.2 | 6.1 | 5.2 | 77.3 | 0.4 |
| **pE 89.0** | 1.5 | 3.9 | 65.3 | 5.3 | 5.1 | 75.7 | 0.4 |
| **pE 88.0** | 1.6 | 9.0 | 76.4 | 5.6 | 5.2 | 77.6 | 0.5 |
| **pE 87.5** | 1.6 | 7.5 | 75.0 | 6.4 | 5.0 | 78.9 | 0.3 |
| **pE 82.0** | 1.2 | 2.2 | 64.6 | 5.0 | 5.0 | 74.7 | 0.4 |
| **pE 81.5** | 1.7 | 7.4 | 78.0 | 5.6 | 5.2 | 78.2 | 0.8 |
| **pE 81.0** | 1.5 | 5.6 | 75.9 | 5.4 | 5.1 | 78.3 | 0.8 |
| **pE 80.0** | 1.3 | 7.1 | 70.7 | 7.5 | 5.2 | 75.9 | 0.7 |
| **pE 79.0** | 1.4 | 4.3 | 77.0 | 20.0 | 5.0 | 79.2 | 0.3* |
| **pE 76.5** | 1.5 | 5.2 | 70.5 | 5.4 | 5.2 | 75.2 | 0.6 |
| **pE 72.5** | 2.1 | 63.2 | 65.2 | 13.7 | 5.6 | 80.0 | 1.2 |
| **pE 72.0** | 1.4 | 18.4 | 66.3 | 11.3 | 5.3 | 76.8 | 0.5 |
| **pE 71.0** | 1.7 | 7.2 | 75.8 | 6.2 | 5.2 | 81.3 | 0.6 |
| **pE 69.0** | 1.6 | 5.6 | 77.9 | 5.7 | 5.0 | 80.2 | 0.5 |
| **pE 68.0** | 1.1 | 7.3 | 68.5 | 5.7 | 5.2 | 72.5 | 0.5 |
| **pE 67.0** | 1.8 | 207.0 | 61.7 | 6.7 | 5.5 | 76.4 | 1.8 |
| **pE 66.5** | 1.7 | 12.7 | 73.5 | 6.4 | 5.2 | 80.3 | 0.8 |
| **pE 66.0** | 1.8 | 31.1 | 70.0 | 8.4 | 5.5 | 83.0 | 1.0 |
| **pE 65.5** | 2.8 | 67.8 | 61.4 | 10.2 | 5.6 | 85.9 | 1.4 |
| **pE 64.0** | 1.6 | 131.7 | 42.5 | 21.3 | 6.0 | 48.4 | 1.3 |
| **pE 62.0** | 1.7 | 137.4 | 65.4 | 9.1 | 5.3 | 85.6 | 1.0 |
| **pE 61.5** | 1.5 | 19.2 | 70.4 | 7.7 | 5.2 | 83.8 | 0.6 |
| **pE 61.0** | 1.7 | 21.8 | 73.6 | 6.8 | 5.0 | 81.2 | 1.1 |
| **pE 60.0** | 1.4 | 15.8 | 65.6 | 7.3 | 5.3 | 78.3 | 0.8 |
| **pE 59.0** | 0.2* | 1.7 | 37.9 | 5.0 | 5.0 | 25.7 | 1.0 |
| **pE 57.0** | 1.4 | 15.6 | 66.1 | 10.0 | 5.2 | 80.1 | 0.6 |
| **pE 56.5** | 1.4 | 7.4 | 73.1 | 6.4 | 5.3 | 82.7 | 0.6 |
| **pE 54.0** | 1.7 | 6.0 | 75.3 | 6.2 | 5.2 | 83.1 | 0.5 |
| **pE 53.5** | 1.4 | 3.8 | 74.7 | 5.7 | 5.1 | 78.8 | 0.7 |
| **pE 51.5** | 1.4 | 9.6 | 70.9 | 7.5 | 5.2 | 81.3 | 0.6 |
| **pE 51.0** | 1.6 | 17.1 | 71.5 | 7.6 | 5.3 | 80.6 | 0.5 |
| **pE 50.0** | 1.1 | 3.5 | 55.0 | 5.8 | 5.3 | 43.2 | 0.6 |
| **pE 47.0** | 0.3 | 2.6 | 53.0 | 5.2 | 5.1 | 33.3 | 0.5 |
| **pE 44.0** | 1.4 | 12.2 | 69.8 | 9.0 | 5.8 | 78.9 | 0.6 |
| **pE 43.5** | 1.2 | 6.6 | 71.2 | 6.1 | 5.2 | 76.0 | 0.4 |
| **pE 40.0** | 0.2* | 5.4 | 38.1 | 5.3 | 5.1 | 28.0 | 0.7 |
| **pE 38.0** | 0.2* | 14.3 | 37.4 | 8.6 | 5.4 | 30.3 | 1.0 |
| **pE 36.0** | 0.2* | 23.2 | 35.8 | 8.8 | 5.3 | 29.6 | 0.4 |

* For values with a *, the lowest detection limit for the given analyte was substitued for the original analysis value, which fell below the lowest level of detection.

| Sample | U/Th (x $10^{-2}$) | Ni/Co | V/Cr | V/(V+Ni) |
|---|---|---|---|---|
| **pE 103.0** | 0.8 | 3.4 | 0.5 | 0.5 |
| **pE 102.0** | 1.0 | 5.9 | 0.3 | 0.5 |
| **pE 101.0** | 1.0 | 5.4 | 1.2 | 0.6 |
| **pE 100.0** | 0.8 | 7.7 | 0.4 | 0.4 |
| **pE 94.0** | 0.5 | 10.6 | 0.7 | 0.5 |
| **pE 89.5** | 0.6 | 9.5 | 0.8 | 0.5 |
| **pE 89.0** | 0.5 | 3.5 | 0.3 | 0.5 |
| **pE 88.0** | 0.7 | 4.0 | 0.6 | 0.5 |
| **pE 87.5** | 0.4 | 5.6 | 0.6 | 0.5 |
| **pE 82.0** | 0.5 | 3.1 | 0.2 | 0.7 |
| **pE 81.5** | 1.0 | 7.9 | 1.3 | 0.5 |
| **pE 81.0** | 1.0 | 13.6 | 1.4 | 0.5 |
| **pE 80.0** | 0.9 | 21.1 | 1.2 | 0.5 |
| **pE 79.0** | 0.3 | 2.6 | 1.3 | 0.5 |
| **pE 76.5** | 0.9 | 11.0 | 0.8 | 0.4 |
| **pE 72.5** | 1.5 | 19.8 | 1.1 | 0.5 |
| **pE 72.0** | 0.7 | 19.6 | 1.2 | 0.5 |
| **pE 71.0** | 0.8 | 10.1 | 2.1 | 0.4 |
| **pE 69.0** | 0.6 | 17.3 | 1.2 | 0.5 |
| **pE 68.0** | 0.7 | 3.7 | 1.2 | 0.5 |
| **pE 67.0** | 2.3 | 18.9 | 1.2 | 0.6 |
| **pE 66.5** | 1.0 | 18.1 | 1.5 | 0.5 |
| **pE 66.0** | 1.2 | 11.2 | 1.0 | 0.4 |
| **pE 65.5** | 1.7 | 10.3 | 0.9 | 0.3 |
| **pE 64.0** | 2.6 | 7.7 | 1.1 | 0.6 |
| **pE 62.0** | 1.1 | 13.5 | 1.7 | 0.6 |
| **pE 61.5** | 0.8 | 13.4 | 1.2 | 0.5 |
| **pE 61.0** | 1.3 | 12.5 | 1.5 | 0.5 |
| **pE 60.0** | 1.1 | 6.6 | 0.8 | 0.6 |
| **pE 59.0** | 3.8 | 0.0 | 1.3 | 1.0 |
| **pE 57.0** | 0.7 | 9.8 | 0.8 | 0.5 |
| **pE 56.5** | 0.7 | 5.3 | 0.4 | 0.4 |
| **pE 54.0** | 0.6 | 25.2 | 0.9 | 0.5 |
| **pE 53.5** | 0.9 | 6.7 | 1.3 | 0.4 |
| **pE 51.5** | 0.8 | 14.5 | 1.2 | 0.6 |
| **pE 51.0** | 0.7 | 9.0 | 0.8 | 0.5 |
| **pE 50.0** | 1.5 | 3.5 | 0.2 | 0.6 |
| **pE 47.0** | 1.6 | 1.2 | 0.8 | 0.6 |
| **pE 44.0** | 0.8 | 2.8 | 0.7 | 0.5 |
| **pE 43.5** | 0.5 | 6.4 | 0.8 | 0.6 |
| **pE 40.0** | 2.3 | 0.0 | 0.6 | 1.0 |
| **pE 38.0** | 3.2 | 1.3 | 1.0 | 0.7 |
| **pE 36.0** | 1.3 | 1.0 | 1.0 | 0.8 |